

NACA RM E55H31



# RESEARCH MEMORANDUM

PERFORMANCE AND COMPONENT FRONTAL AREAS OF A  
HYPOTHETICAL TWO-SPOOL TURBOJET ENGINE FOR  
THREE MODES OF OPERATION

By James F. Dugan, Jr.

Lewis Flight Propulsion Laboratory  
CLASSIFICATION CHANGED  
Cleveland, Ohio

UNCLASSIFIED

Authority of *NASA SRA 11* Date *12-1-97*  
*Effective*  
*7B 2-1-60*

CLASSIFIED DOCUMENT

This material contains information which is classified as CONFIDENTIAL within the meaning of the espionage laws, Title 18, U.S.C., Sec. 793 and 794, the transmission or revelation of which in any manner to an unauthorized person is prohibited by law.

## NATIONAL ADVISORY COMMITTEE FOR AERONAUTICS

WASHINGTON  
December 19, 1955



UNCLASSIFIED

## NATIONAL ADVISORY COMMITTEE FOR AERONAUTICS

RESEARCH MEMORANDUMPERFORMANCE AND COMPONENT FRONTAL AREAS OF A HYPOTHETICAL TWO-  
SPOOL TURBOJET ENGINE FOR THREE MODES OF OPERATION

By James F. Dugan, Jr.

## SUMMARY

A hypothetical two-spool turbojet engine having a design compressor pressure ratio of 7.0 and a design inner-turbine inlet temperature of 2500° R is operated over a range of flight conditions for each of three operating modes. At sea level, the flight Mach number is varied from 0 to 0.9, while in the stratosphere, Mach number is varied from 0.9 to 2.8. For all three modes, inner-turbine inlet temperature is maintained constant at 2500° R. For mode I operation, outer-spool mechanical speed is maintained constant at its design value. For mode II, inner-spool mechanical speed is maintained constant at its design value. For mode III, outer-compressor equivalent speed is maintained constant at 110 percent of design for all engine-inlet temperatures less than 567° R; for higher inlet temperatures, outer-compressor mechanical speed is maintained constant at 115 percent design. Engine performance with afterburning and with the afterburner inoperative and component frontal areas are calculated for each operating mode.

Mode I engine performance is better than that for mode II over most of the flight range. In general, thrust values are higher, while specific fuel consumption for the two modes is about the same. The inner-spool centrifugal stress for mode I is 12 percent higher than for mode II, while the outer-spool centrifugal stress is 12 percent higher for mode II than for mode I. At Mach 2.8, the combustor frontal area for mode I is 6 percent larger than the compressor frontal area. For the range of flight conditions considered, the combustor frontal area for mode II is always smaller than the compressor frontal area. The maximum afterburner frontal area for modes I and II is about 19 percent greater than the compressor frontal area. At Mach 2.36 with the afterburner inoperative, the ratio of exhaust-nozzle-exit area for complete expansion to compressor frontal area is 1.59 for mode I, compared with 1.32 for mode II; with afterburning, the ratios are 2.16 for mode I, compared with 1.78 for mode II.

Engine performance for mode III operation is better than that for mode I. Thrust for mode III is higher, while specific fuel consumption

UNCLASSIFIED

for mode III is less than that for mode I. The maximum outer-spool centrifugal stress for mode III is 32 percent higher than that for mode I, while the inner-spool centrifugal stress is the same for modes III and I. At Mach 2.8, the combustor frontal area for mode III is 11.5 percent larger than the compressor frontal area, while that for mode I is only 6 percent larger. The afterburner frontal area for mode III is 35 percent greater than the compressor frontal area, while that for mode I is 18.5 percent greater. At Mach 2.8 with the afterburner inoperative, the ratio of exhaust-nozzle-exit area for complete expansion to compressor frontal area is 2.13 for mode III compared with 1.92 for mode I; with afterburning, the ratios are 3.05 for mode III compared with 2.62 for mode I.

3820

### INTRODUCTION

A gas-turbine engine is designed for a specific flight condition, such as sea-level take-off. At this condition, the engine components operate efficiently at the desired values of compressor-inlet equivalent specific weight flow, turbine- to compressor-temperature ratio, and compressor total-pressure ratio. Component efficiencies, compressor-inlet equivalent specific weight flow, turbine- to compressor-temperature ratio, and compressor total-pressure ratio vary at other flight conditions. These variations, which determine the engine performance at other than design flight conditions, depend on the mode of engine operation. The operating mode also affects the location of the component operating lines on the performance maps. Over the full range of flight conditions, the compressor should operate at a high level of efficiency and specific weight flow with adequate surge margin to permit acceptable accelerations and stable operation. The turbine should operate at a high level of efficiency for all flight conditions, and operation very close to limiting loading should be avoided. The velocities in the combustor and afterburner should not exceed specified limits.

Any gains in engine performance that result from a particular mode of operation should be evaluated by considering the concomitant effects on the size and weight of the various components. For example, from the standpoint of engine net thrust, the compressor specific weight flow should be as high as possible at each flight condition. A higher specific weight flow, however, means larger frontal areas for combustor, afterburner, and exhaust nozzle for a given set of aerodynamic and structural limits. Larger components result in an engine weight increase and a possible reduction in net thrust per unit engine frontal area or net thrust per pound of engine weight over some portion of the operating range.

This report compares the performance, centrifugal stresses, and component frontal areas of a hypothetical two-spool turbojet engine for three modes of operation. The engine considered has a design pressure ratio of 7.0 and a design inner-turbine inlet temperature of 2500° R.

The maximum thrust at any flight condition is achieved by operating the engine at maximum values of component efficiencies, compressor inlet equivalent weight flow, and turbine- to compressor-temperature ratio, and at a compressor total-pressure ratio that depends on the flight condition, the turbine- to compressor-temperature ratio, and the component efficiencies. However, for a two-spool turbojet engine having fixed-geometry compressors and turbines, the performance at any flight condition is fixed by specifying two independent engine quantities such as inner-turbine inlet temperature and engine speed. The maximum turbine- to compressor-temperature ratio (consistent with the engine strength requirements) is achieved by specifying an inner-turbine inlet temperature of 2500° R (the design value) during all flight conditions for all three operating modes. An engine speed specification is desired so that maximum compressor-inlet equivalent weight flow will result at each flight condition.

For mode I operation, the mechanical speed of the outer-spool is assigned to be constant at its design value for all flight conditions. For mode II operation, the inner-spool mechanical speed is assigned to be constant at its design value for all flight conditions. Although these two modes yield the same design performance, the performance at other than design conditions will differ because of the different variations in component efficiencies, compressor total-pressure ratio, and compressor equivalent specific weight flow.

For mode III operation, the mechanical speed of the outer spool is varied so that either the outer-spool equivalent speed is 110 percent of design or the mechanical speed of the outer spool is 115 percent of design. Because of the higher outer-spool equivalent speed, the compressor equivalent weight flow will be higher for mode III than for mode I. Therefore, the thrust at each flight condition is expected to be higher for mode III than for mode I. The values of outer-spool mechanical speed and equivalent weight flow entering the combustor, afterburner, and exhaust nozzle will be greater for mode III than for mode I. Therefore, the values of outer-spool centrifugal stress and component frontal area will be higher for mode III than for mode I.

#### METHOD OF ANALYSIS

After compressor and turbine maps are obtained analytically, the gas-generator pumping characteristics are obtained by matching the compressor, combustor, and turbine components. Engine performance with afterburning and with the afterburner inoperative is calculated for three modes of operation over a range of flight conditions. Operating lines for each mode are located on each of the compressor and turbine performance maps.

The variations of outer-spool equivalent speed, outer-spool mechanical speed, inner-spool mechanical speed, and outer-spool equivalent weight flow with flight condition are found.

The areas of the engine components are calculated from assigned aerodynamic and structural limits and the engine performance for each operating mode. The compressor and turbine frontal areas are based on the design-point cycle calculations and given limits so that they are the same for all three operating modes. The frontal areas of the combustor, afterburner, and exhaust nozzle for complete expansion are based on engine performance over the full range of flight conditions so that the maximum areas compatible with the assigned limits vary with operating mode. No attempt is made to calculate engine weight.

3820

### Description of Engine

Design conditions. - A cross section of a two-spool turbojet engine with an afterburner and the designated axial stations are shown in figure 1. (All symbols are defined in appendix A.) The two-spool-engine design conditions for sea-level operation at a Mach number of zero are as follows:

|  |       |
|--|-------|
| Over-all compressor pressure ratio . . . . .                         | 7.0   |
| Outer-compressor equivalent weight flow, lb/sec . . . . .            | 150   |
| Outer- and inner-compressor pressure ratio . . . . .                 | 2.646 |
| Outer- and inner-compressor polytropic efficiency, percent . . . . . | 90    |
| Inner-turbine inlet temperature, °R . . . . .                        | 2500  |
| Inner-turbine equivalent specific work, Btu/lb . . . . .             | 12.8  |
| Inner- and outer-turbine adiabatic efficiency, percent . . . . .     | 87    |
| Outer-turbine equivalent specific work, Btu/lb . . . . .             | 10.3  |
| Afterburner temperature, °R . . . . .                                | 3500  |

Component performance. - The outer- and inner-compressor performance maps are shown in figures 2(a) and (b). Each map was obtained in three steps: by calculating the "backbone" or line of maximum efficiency, the compressor stall-limit line, and constant-speed lines. This procedure and the required curves are presented in reference 1.

The inner- and outer-turbine performance maps (figs. 2(c) and (d)) were obtained from the one-stage-turbine performance map of reference 2, as described in reference 1.

### Pumping Characteristics

The pumping characteristics of a gas generator, as used in this report, are defined as the relations among the following quantities:  $T_4/T_1$ ,  $N_0/\sqrt{\theta_1}$ ,  $N_1/\sqrt{\theta_1}$ ,  $w_1\sqrt{\theta_6}/\delta_6$ ,  $P_6/P_1$ ,  $T_6/T_1$ , and  $f/\theta_1$ . The pumping characteristics are obtained by plotting the compressor and turbine component

performance in terms of quantities suitable for matching and relating the performances of the compressors, combustor, and turbines in order to satisfy the matching relations. This was achieved by matching the inner compressor, primary combustor, and inner turbine to obtain inner-spool performance and then matching the inner spool with the outer compressor and outer turbine. Matching procedures, similar to those described in reference 3, are presented in appendix B.

### Modes of Operation

Before the performance of a turbojet engine at a given flight Mach number and altitude can be calculated, the manner in which the engine is operated must be specified. For equilibrium operation, two engine quantities must be specified. Three modes of operation are considered for the hypothetical two-spool turbojet. For all three modes, the inner-turbine inlet temperature is assigned to be  $2500^{\circ}$  R, the design value. (Lower thrust values would result from specifying a lower inner-turbine inlet temperature.) For mode I operation, the second quantity assigned is outer-spool mechanical speed; this is assigned to be constant at its design value for all operating conditions. Inner-spool mechanical speed for mode II is assigned to be constant at its design value for all flight conditions. For sea-level operation at a Mach number of zero, then, the two-spool engine operates at design conditions for modes I or II. For mode III operation, the outer-spool equivalent speed is assigned to be constant at 110 percent design for all values of engine-inlet temperature less than  $567^{\circ}$  R. The two-spool engine does not operate at its design conditions for mode III sea-level operation at a Mach number of zero. The values of compressor equivalent weight flow and over-all compressor pressure ratio are 170 pounds per second and 7.98, respectively, instead of 150 pounds per second and 7.0. At sea level, engine-inlet temperature increases from  $518.7^{\circ}$  to  $567^{\circ}$  R as flight Mach number increases from 0 to 0.68. In the stratosphere, engine-inlet temperature is less than  $567^{\circ}$  R for flight Mach numbers less than 1.51. For all inlet temperatures greater than  $567^{\circ}$  R (flight Mach numbers greater than 0.68 at sea level and 1.51 in the stratosphere), outer-spool mechanical speed is held constant at 115 percent design. At an inlet temperature of  $567^{\circ}$  R, an outer-spool mechanical speed of 115 percent design corresponds to an outer-spool equivalent speed of 110 percent design.

Operation is considered at sea level for flight Mach numbers from 0 to 0.9 and in the stratosphere from 0.9 to 2.8, except for mode II operation. The minimum flight Mach number in the stratosphere for mode II is 1.08. At this flight condition, outer-spool equivalent speed is 110 percent of its design value. The maximum flight Mach number for mode II is 2.36; at this flight condition, outer-spool equivalent speed is 70 percent of its design value. In order to extend the minimum flight Mach number in the stratosphere from 1.08 to 0.9, the outer-compressor performance

at speeds greater than 110 percent design would have to be estimated. The curves of reference 1, from which compressor performance is estimated, do not exceed 110 percent design. In order to extend the maximum flight Mach number in the stratosphere from 2.36 and 2.8, outer-compressor performance at speeds less than 70 percent design and outer-turbine performance at speeds less than 83 percent design would have to be estimated. This was not done because it was believed that the range covered was sufficient to make the comparisons between modes I and II.

#### Component Operating Lines

Operating lines are located on the compressor and turbine component maps by finding the variations of  $T_4/T_1$  and  $N_o/\sqrt{\theta_1}$  with flight condition and then reading the component map variables from gas-generator plots of the variables against  $T_4/T_1$  for constant values of  $N_o/\sqrt{\theta_1}$ .

For all three modes, the engine-inlet temperature at each flight condition is calculated from

$$T_1 = t_0 \left( 1 + \frac{\gamma-1}{2} M_0^2 \right) \quad (1)$$

where  $t_0$  is the ambient temperature at the specified altitude and  $M_0$  is the specified flight Mach number. Since  $T_4$  is assigned to be constant, the variation of  $T_4/T_1$  with flight condition can be calculated. For mode I operation, for which  $N_o$  is assigned, the equivalent-speed variation with flight condition is calculated from

$$\frac{N_o}{\sqrt{\theta_1}} = N_o \left( \frac{518.7}{T_1} \right)^{1/2} \quad (2)$$

For mode II operation, an iteration procedure was used to find the variation of  $N_o/\sqrt{\theta_1}$  with flight condition. The variation of  $N_i/\sqrt{\theta_1}$  with flight condition is found from

$$\frac{N_i}{\sqrt{\theta_1}} = N_i \left( \frac{518.7}{T_1} \right)^{1/2} \quad (3)$$

where  $N_i$  is assigned to be the design value for all flight conditions. For each flight condition, the value of  $N_o/\sqrt{\theta_1}$  is found as follows:

(1) Values of  $T_4/T_1$  and  $N_1/\sqrt{\theta_1}$  are found from the variation of these variables with flight condition.

(2) Trial values of  $N_0/\sqrt{\theta_1}$  and  $w_1\sqrt{\theta_6}/\delta_6$  are read from the pumping-characteristic plot,  $T_4/T_1$  against  $w_1\sqrt{\theta_6}/\delta_6$  for constant  $N_0/\sqrt{\theta_1}$ , for the known  $T_4/T_1$ .

(3) A value of  $N_1/\sqrt{\theta_1}$  is read from the gas-generator plot,  $N_1/\sqrt{\theta_1}$  against  $w_1\sqrt{\theta_6}/\delta_6$  for constant  $N_0/\sqrt{\theta_1}$ , for the trial values of  $N_0/\sqrt{\theta_1}$  and  $w_1\sqrt{\theta_6}/\delta_6$  from step (2). If this value does not equal the known  $N_1/\sqrt{\theta_1}$  value from step (1), steps (2) and (3) are repeated until agreement is reached. This iteration procedure gives more accurate results than the more direct method of reading  $N_0/\sqrt{\theta_1}$  values from a gas-generator plot,  $N_1/\sqrt{\theta_1}$  against  $T_4/T_1$  for constant  $N_0/\sqrt{\theta_1}$ , for the known values of  $T_4/T_1$  and  $N_1/\sqrt{\theta_1}$  at each flight condition.

For mode III operation, the  $N_0/\sqrt{\theta_1}$  variation with flight condition is calculated from equation (2) when  $N_0$  is assigned to be 115-percent design. For part of the flight range, a constant equivalent speed  $N_0/\sqrt{\theta_1}$  of 110-percent design is assigned. Gas-generator plots of  $P_2/P_1$ ,  $w_1\sqrt{\theta_1}/\delta_1$ ,  $P_3/P_2$ ,  $w_2\sqrt{\theta_2}/\delta_2$ ,  $(H_4 - H_5)/\theta_4$ ,  $w_4N_1/\delta_4$ ,  $(H_5 - H_6)/\theta_5$ , and  $w_5N_0/\delta_5$  against  $T_4/T_1$  for constant  $N_0/\sqrt{\theta_1}$  are made. For each flight condition, the compressor and turbine variables are read for the known values of  $T_4/T_1$  and  $N_0/\sqrt{\theta_1}$ . For each operating mode, operating lines are plotted on the compressor and turbine component maps.

### Engine Performance

Thrust and specific-fuel-consumption values are calculated for afterburning and inoperative-afterburner operation. The afterburning temperature is assigned to be constant at its design value, 3500° R.

The following procedure is used to calculate engine performance for each operating mode:

(1) For an assigned flight condition, values of  $T_4/T_1$  and  $N_0/\sqrt{\theta_1}$  are found as discussed previously.

(2) Values of  $w_1\sqrt{\theta_6}/\delta_6$ ,  $P_6/P_1$ ,  $T_6/T_1$ , and  $f/\theta_1$  are read from the pumping-characteristic curves for the values of  $T_4/T_1$  and  $N_0/\sqrt{\theta_1}$ .

(3) The inlet total-pressure-recovery ratio  $P_1/P_0$  is read from figure 2(e), a calculated plot of  $P_1/P_0$  against  $M_0$  for a variable-geometry inlet having two adjustable wedges and a by-pass duct.

(4) Exhaust-nozzle pressure ratio is calculated from

$$\frac{P_7}{P_0} = \frac{P_0}{P_0} \frac{P_1}{P_0} \frac{P_6}{P_1} \frac{P_7}{P_6} \quad (4)$$

where

$$\frac{P_0}{P_0} = \left(1 + \frac{\gamma-1}{2} M_0^2\right)^{\frac{\gamma}{\gamma-1}} \quad (5)$$

$P_7/P_6 = 0.96$  for inoperative-afterburner operation

$P_7/P_6 = 0.94$  for afterburning operation

(5) Jet velocity is calculated from

$$V_j = C_V \sqrt{\frac{2gR\gamma_7}{\gamma_7-1} T_7 \left[1 - \left(\frac{P_0}{P_7}\right)^{\frac{\gamma_7-1}{\gamma_7}}\right]} \quad (6)$$

where  $C_V = 0.96$ ,  $T_7 = T_6$  for inoperative-afterburner operation, and  $T_7 = 3500^\circ \text{R}$  for afterburning operation.

(6) Net thrust is calculated from

$$F_n = \frac{w_1}{g} [(1+f) V_j - V_0] \quad (7)$$

where  $w_1$  is calculated from values of  $\bar{w}_1 \sqrt{\theta_6/\delta_6}$ ,  $T_6/T_1$ ,  $P_6/P_1$ ,  $P_1$ , and  $T_1$ ;  $V_0$  is calculated from

$$V_0 = M_0 \sqrt{\gamma g R t_0} \quad (8)$$

and the fuel-air ratio is calculated from values of  $f/\theta_1$  and  $T_1$  for inoperative-afterburner operation. For afterburning, the value of fuel-air ratio for the afterburner is found by using figure 2 of reference 4.

In calculating the total fuel-air ratio, combustor efficiency is taken equal to 0.95 and afterburner efficiency equal to 0.90. The fuel is assumed to have a lower heating value of 18,700 Btu per pound and a hydrogen-carbon ratio of 0.175.

(7) Specific fuel consumption is calculated from

$$\text{sfc} = \frac{3600 f}{\frac{F_n}{W_1}} \quad (9)$$

#### Component Areas

The component frontal areas of the hypothetical two-spool turbojet engine were computed for the following design values:

|   |      |
|---|------|
| Air flow per unit frontal area at station 1, lb/(sec)(sq ft) . . . . .                | 35   |
| Outer-compressor tip speed, ft/sec . . . . .  | 1100 |
| Outer-compressor entrance axial Mach number . . . . .                                 | 0.6  |
| Ratio of inner- to outer-compressor first-rotor tip relative<br>Mach number . . . . . | 1.0  |
| Ratio of inner- to outer-compressor inlet axial velocity . . . . .                    | 1.0  |
| Inner- and outer-compressor exit tangential velocity, ft/sec . . . . .                | 0    |
| Inner-turbine exit axial-velocity ratio, $V_{x,5}/a_{cr,5}$ . . . . .                 | 0.5  |
| Number of inner-turbine stages . . . . .  | 1    |
| Inner-turbine loading parameter, $Jg(H_4 - H_5)/U_{h,5}^2$ . . . . .                  | 2.1  |
| Outer-turbine exit axial-velocity ratio, $V_{x,6}/a_{cr,6}$ . . . . .                 | 0.5  |
| Number of outer-turbine stages . . . . .  | 1    |
| Outer-turbine loading parameter, $Jg(H_5 - H_6)/U_{h,6}^2$ . . . . .                  | 2.1  |
| Primary-combustor reference velocity, ft/sec . . . . .                                | 200  |
| Primary-combustor hub-tip radius ratio . . . . .                                      | 0.4  |
| Afterburner velocity, ft/sec . . . . .  | 550  |

Outer-compressor frontal area was calculated from the values of air flow and air flow per unit frontal area; inner-compressor frontal area was assigned equal to outer-compressor frontal area. Values of outer-compressor tip speed and entrance axial Mach number yielded values of rotor tip relative Mach number and hub-tip radius ratio. Guide vanes were not used. Inner-spool tip speed and inner-compressor first-rotor hub-tip radius ratio were calculated from the values of equivalent weight flow, temperature, axial velocity, and rotor tip relative Mach number at the entrance of the inner spool.

The exit-annulus area of each turbine was computed from design point cycle calculations which gave values of turbine-exit equivalent weight

flow, and the selected value of turbine-exit axial-velocity ratio, which gave values of turbine-exit equivalent specific weight flow. The hub radius of each turbine was calculated from design values of turbine specific work, stage loading parameter, and angular velocity. This hub-radius value, together with the value of annulus area, determined the frontal area and exit hub-tip radius ratio of each turbine. Constant rotor tip radius was assumed for each turbine. Rotor blade hub centrifugal stresses were calculated for assigned values of blade taper factor, 0.7, and density of material, 490 pounds per cubic foot.

At each flight condition, the primary-combustor frontal area was calculated from the following equations:

$$\frac{w_3 \sqrt{\theta_3}}{\delta_3} = \frac{w_1 \sqrt{\theta_1}}{\delta_1} \frac{\sqrt{T_3/T_1}}{P_3/P_1} \left( \frac{w_3}{w_1} \right) \quad (10)$$

$$\frac{V_3}{a_{T,3}} = \frac{V_3}{\sqrt{\gamma_3 g R T_3}} \quad (11)$$

$$\frac{\rho_3}{\rho_{T,3}} = \left[ 1 - \frac{\gamma_3 - 1}{2} \left( \frac{V_3}{a_{T,3}} \right)^2 \right]^{\frac{1}{\gamma_3 - 1}} \quad (12)$$

$$\frac{w_3 \sqrt{\theta_3}}{\delta_3 A_{an,3}} = 2116 \sqrt{\frac{\gamma_3 g}{518.7 R}} \left( \frac{\rho_3}{\rho_{T,3}} \right) \left( \frac{V_3}{a_{T,3}} \right) \quad (13)$$

$$A_{an,3} = \frac{\frac{w_3 \sqrt{\theta_3}}{\delta_3}}{\frac{w_3 \sqrt{\theta_3}}{\delta_3 A_{an,3}}} \quad (14)$$

$$A_{F,3} = \frac{A_{an,3}}{(1 - z_{h,3}^2)} \quad (15)$$

The values of  $V_3$  in equation (11) and  $z_{h,3}$  in equation (15) were assigned to be 200 feet per second and 0.4, respectively.

The preceding equations with station 6a replacing station 3 were used to calculate the afterburner frontal area at each flight condition. The value  $V_{6a}$  is assigned to be 550 feet per second and  $z_{h,6a}$  to be zero.

At each flight condition, the exhaust-nozzle-exit area required for complete expansion was calculated from the following equations:

$$\left(\frac{w\sqrt{\theta}}{\delta}\right)_8 = \left(\frac{w_1\sqrt{\theta_6}}{\delta_6}\right) \frac{(1+f)\sqrt{T_8/T_6}}{P_8/P_6} \quad (16)$$

$$\left(\frac{w\sqrt{\theta}}{\delta A}\right)_8 = 2116 \sqrt{\frac{\gamma_8}{518.7 R}} M_8 \left(1 + \frac{\gamma_8 - 1}{2} M_8^2\right)^{-\frac{(\gamma_8 + 1)}{2(\gamma_8 - 1)}} \quad (17)$$

$$A_8 = \frac{\left(\frac{w\sqrt{\theta}}{\delta}\right)_8}{\left(\frac{w\sqrt{\theta}}{\delta A}\right)_8} \quad (18)$$

where  $M_8$  is found from the values of  $P_8/P_0$  and  $\gamma_8$ . For operation without afterburning,  $T_8/T_6$  equaled 1.0 and  $P_8/P_6$  was assigned equal to 0.96. For operation with afterburning,  $T_8 = 3500^\circ R$  and  $P_8/P_6$  was assigned equal to 0.94. Exhaust-nozzle-throat areas were calculated from the above equations with station 7a replacing station 8 and  $M_{7a} = 1.0$ . The total-pressure and total-temperature values at station 7a were assumed equal to the values at station 8.

## RESULTS AND DISCUSSION

### Component Operating Lines

The operating lines for the three modes of operation are shown on the two-spool turbojet compressor and turbine component maps (fig. 3). Each operating line corresponds to the full range of flight conditions considered, but only the minimum and maximum flight Mach numbers in the stratosphere are noted in the tables.

Outer compressor. - All three operating lines on the outer-compressor performance map are parallel to the stall-limit line (fig. 3(a)). For modes I and II, the operating lines pass through the maximum-efficiency region. The operating line for mode III lies closer to the stall-limit line because the compressor and turbine components were sized for the zero Mach number sea-level conditions of modes I and II. The components could be designed for other conditions so that the mode III operating line would pass through the maximum-efficiency range, and the margin between the operating line and the stall-limit line would be improved.

Inner compressor. - The inner compressor operates at peak efficiency only at speeds  $N_1/\sqrt{\theta_2}$  near design, because the slopes of the operating lines on the inner-compressor performance map are greater than the slope of the stall-limit line (fig. 3(b)). For all three modes, the inner-compressor equivalent-speed range is less than the corresponding outer-compressor equivalent-speed range. The minimum inner-compressor efficiency is 0.71 for mode III operation, 0.77 for mode I operation, and 0.85 for mode II operation. However, these minimum-efficiency points correspond to different flight Mach numbers in the stratosphere - 2.80 for modes I and III and 2.36 for mode II. In order to evaluate the three modes of operation, comparisons will be made of various quantities plotted against flight Mach number for the three modes. For this engine, neither compressor is restricted by its stall-limit line for any of the operating modes.

Inner turbine. - The operating lines for the three modes of operation are shown on the inner-turbine map (fig. 3(c)). The design value of equivalent specific work is not exceeded for any of the operating modes. For mode I, specific work is constant at its design value while the flow parameter varies from 25.5 to 27.4. For mode II, the flow parameter is constant at its design value while specific work varies from 12.5 to 12.8 Btu per pound. For mode III, specific work is constant at its design value while the flow parameter varies from 25.6 to 27.9 Btu per pound. For all three operating modes, the inner turbine operates very close to its design point for the full range of flight conditions. Turbine efficiency varies only slightly between 0.87 and 0.88.

Outer turbine. - Operating lines for the three modes of operation are shown on the outer-turbine performance map (fig. 3(d)). For mode I, specific work varies from 10.0 to 11.4 while flow parameter is constant at its design value. Efficiency is nearly constant at 0.87. For mode II operation, specific work varies from 8.3 to 11.4 while flow parameter varies from 28.2 to 35.8. Efficiency is nearly constant at 0.87. For mode III operation, specific work varies from 10.6 to 16.4 while flow parameter varies from 34.7 to 38.9. For operation during which equivalent speed  $N_0/\sqrt{\theta_5}$  varies, the turbine efficiency varies between 0.87 and 0.85. For operation during which equivalent speed  $N_0/\sqrt{\theta_5}$  is constant, the turbine efficiency varies between 0.85 and about 0.79. At the high

Mach number end of the mode III operating line, operation is very close to the estimated limiting-loading line. For operating modes I and II, the outer-turbine efficiency is nearly constant, while for mode III, it varies from 0.87 to about 0.79.

#### Engine Speed Variations

3820 Equivalent speed of outer compressor. - The outer-compressor equivalent speed variations serve to indicate the engine equivalent weight flow variations and hence the engine thrust variations. The variation of outer-compressor equivalent speed with flight Mach number for the three operating modes is shown in figure 4. The equivalent speed values for mode III are highest over the entire flight range. The values for mode I are higher than for mode II except for the Mach number range 0.9 to 1.3 in the stratosphere. Because the calculations were limited to the outer-compressor equivalent speed range 70 to 110 percent design, the range of flight Mach numbers in the stratosphere for mode II operation extends from 1.08 to 2.36.

Outer-spool mechanical speed. - The variation of outer-spool mechanical speed with flight Mach number is shown in figure 5(a). The outer-spool mechanical speed variations indicate the centrifugal stress level in the outer-spool compressor and turbine because centrifugal stress is proportional to the square of the rotational speed. An engine is constructed to withstand safely the highest stress level encountered during the flight plan. For mode I, the outer-spool speed is specified to be constant over the entire flight range. For mode II, the highest outer-spool speed occurs at a flight Mach number of 1.08 in the stratosphere. The peak value of 106-percent design would result in outer-spool stresses 12 percent higher than for mode I. For mode III, the mechanical speed was allowed to increase to a value of 115-percent design which prevails over a large part of the flight range. This results in a maximum outer-spool stress level 32 percent higher than for mode I. Because a heavier structure is required to withstand these higher stresses, improvements in performance for mode III would be partially offset by the increased weight of the outer spool.

Inner-spool mechanical speed. - The inner-spool mechanical speed variation with flight Mach number is shown in figure 5(b). For mode II operation, the inner-spool speed is specified to be constant over the entire flight range. The maximum value of inner-spool speed for modes I and III is about 6 percent higher than for mode II. The stress level in the inner-spool compressor and turbine would be 12 percent higher for modes I and III than for mode II. From a centrifugal stress consideration, the inner-spool for mode III operation would not be heavier than for mode I operation so that any gains in thrust for mode III over mode I would not be lessened by inner-spool weight increases.

~~CONFIDENTIAL~~

### Weight-Flow Variations

The variation of engine equivalent weight flow with flight Mach number for the three modes of operation is shown in figure 6. These weight-flow variations influence the engine thrust variations because thrust is proportional to weight flow.

At sea level, the weight flow for mode I operation is as great or greater than that for mode II. At Mach 0.9, equivalent weight flow is about 14 percent greater for mode I than for mode II. In the stratosphere, mode I weight flow exceeds mode II weight flow for all Mach numbers greater than about 1.3, while at lower Mach numbers, weight flow for mode II is greater. At Mach 2.36, mode I weight flow is about 19 percent greater than that for mode II. At Mach 1.08, mode II weight flow is about 10 percent higher.

For the entire flight range, the greatest weight flow is achieved for mode III operation. At sea level, the improvement over the weight flow for mode I varies from 13 to 19 percent. In the stratosphere the improvement is 6 to 20 percent. Over much of the flight range, the outer-spool equivalent speed for mode III operation is greater than design. Therefore, the weight-flow (and thrust) comparison between modes III and I depends greatly on the overspeed weight-flow characteristics of the outer compressor. For this particular engine, the equivalent weight flow for mode III operation at 110 percent of the design outer-spool equivalent speed is 112 to 117 percent of the design equivalent weight flow. For other engines having high design values of inlet axial Mach number and rotor tip relative Mach number, the increase in overspeed equivalent weight flow might be considerably less. For such an engine, the gains in engine thrust for mode III over mode I would be less than those discussed in the following section.

### Engine Performance

With inoperative afterburner. - Engine performance with the afterburner inoperative for the three modes of operation is shown in figure 7. In figure 7(a) equivalent net thrust as percent design is plotted against flight Mach number. The design value of net thrust is 11,300 pounds. At sea level, thrust for mode I operation is as great or greater than the thrust for mode II. At Mach 0.9, mode I thrust is about 13 percent greater. In the stratosphere, mode I thrust exceeds mode II thrust for all Mach numbers greater than about 1.3, while at lower Mach numbers, thrust for mode II exceeds. At Mach 2.36, mode I thrust is greater than mode II thrust by about 20 percent. At Mach 1.08, mode II thrust is about 10 percent greater.

For the entire flight range, the greatest thrust is achieved for mode III operation. At sea level, the improvement over the thrust for mode I varies from 15 to 21 percent. In the stratosphere, the improvement is 6 to 18 percent.

Specific fuel consumption sfc as percent design is plotted against flight Mach number  $M_0$  in figure 7(b). The design value of specific fuel consumption is 1.166. At sea level, mode I specific fuel consumption is less than or equal to that for mode II. At Mach 0.9, mode I sfc is about 3 percent less than that for mode II. In the stratosphere, mode I sfc is less over part of the  $M_0$  range while mode II sfc is less for other parts. The maximum difference between mode I and mode II sfc is about 3 percent. At sea level, mode III sfc is 3 to 5 percent less than mode I sfc, while in the stratosphere, the difference is 0.5 to 4 percent.

With afterburning. - The trends for engine performance with afterburning (fig. 8) are similar to the trends for engine performance with the afterburner inoperative. At Mach 0.9 at sea level, mode I thrust is 16 percent greater than mode II thrust (fig. 8(a)). At Mach 2.36 in the stratosphere, mode I thrust is 23 percent greater than mode II thrust. At sea level, mode III thrust is 16 to 22 percent greater than mode I thrust and in the stratosphere, 8 to 22 percent.

Over most of the flight range, sfc for modes I and II is about the same (fig. 8(b)). At all Mach numbers less than 2.65, mode III sfc is less than mode I sfc by 0 to 3 percent. At Mach 2.8, mode I sfc is about 1 percent less than mode III sfc.

#### Component Areas

Compressor and turbine frontal areas. - The outer and inner compressor of the hypothetical two-spool turbojet engine each has a frontal area of 4.286 square feet. The frontal areas of the other components will be referred to this compressor frontal area. The inner-turbine frontal area is about 12 percent smaller than the compressor frontal area, while that of the outer turbine is about 11 percent larger. Outer-turbine frontal area would be reduced and inner-turbine frontal area increased if the design value of outer-compressor pressure ratio were reduced and the design value of inner-compressor pressure ratio increased.

The compressor and turbine design values calculated from the assigned component design limits are as follows:

|   |        |
|---|--------|
| Outer- and inner-compressor frontal area, sq ft . . . . .       | 4.286  |
| Outer-compressor first-rotor tip relative Mach number . . . . . | 1.184  |
| Outer-compressor hub-tip radius ratio . . . . .                 | 0.397  |
| Inner-compressor tip speed, ft/sec. . . . .                     | 1357   |
| Inner-compressor first-rotor hub-tip radius ratio . . . . .     | 0.766  |
| Inner-turbine frontal area, sq ft . . . . .                     | 3.788  |
| Inner-turbine-exit hub-tip radius ratio . . . . .               | 0.671  |
| Inner-turbine centrifugal stress at rotor hub, psi . . . . .    | 33,100 |
| Outer-turbine frontal area, sq ft . . . . .                     | 4.739  |
| Outer-turbine-exit hub-tip radius ratio . . . . .               | 0.634  |
| Outer-turbine centrifugal stress at rotor hub, psi . . . . .    | 29,600 |

Combustor frontal area. - Combustor frontal area is plotted against flight Mach number for the three operating modes in figure 9(a). For each operating mode, the maximum combustor frontal area occurs at the highest flight Mach number. At Mach 2.8, the combustor frontal area for mode I is about 6 percent larger than the compressor frontal area. For the range of flight conditions considered, the combustor frontal area for mode II is always smaller than the compressor frontal area. At Mach 2.8, the combustor frontal area for mode III is 11.5 percent larger than the compressor frontal area.

Afterburner frontal area. - The variation of afterburner frontal area with flight Mach number for the three modes of operation is shown in figure 9(b). The maximum frontal areas of the afterburners for modes I, II, and III are 18.5, 19, and 35 percent greater than the compressor frontal area.

Exhaust-nozzle-throat area. - The variation of exhaust-nozzle-throat area with flight Mach number is shown in figure 10. If the variation in exhaust-nozzle-throat area is slight, no control of that area would be needed. If the variation is large, a control would be required. For mode I operation with the afterburner inoperative, the throat area of the exhaust nozzle must vary from 49.8 to 51.5 percent of the compressor frontal area (fig. 10(a)). For mode II, the variation is from 46.6 to 51.7 percent, and for mode III from 50.6 to 59.5 percent.

For operation with afterburning (fig. 10(b)) the throat area variation is from 68.0 to 70.4 percent for mode I, from 62.1 to 70.9 percent for mode II, and from 69.2 to 82.3 percent for mode III.

Exhaust-nozzle-exit area. - The variation in exhaust-nozzle-exit area for complete expansion with flight Mach number for the three modes of operation is shown in figure 11. To obtain complete expansion in the exhaust nozzle for engine operation with the afterburner inoperative, nozzle-exit areas greater than compressor frontal area are required for flight Mach numbers greater than about 1.3 to 1.7, depending on the mode of engine operation (fig. 11(a)). At Mach 2.36, the ratio of nozzle-exit

area to compressor frontal area is 1.59 for mode I compared with 1.32 for mode II. At Mach 2.8, the ratio is 2.13 for mode III compared with 1.92 for mode I. If the exhaust-nozzle-exit area is made equal to the compressor frontal area, the net thrust at Mach 2.8 is reduced 15 percent for mode III operation and 11 percent for mode I operation.

For engine operation with afterburning (fig. 11(b)), nozzle-exit areas greater than compressor area are required for all flight in the stratosphere. At Mach 2.36, the ratio of nozzle-exit area to compressor frontal area is 2.16 for mode I compared with 1.78 for mode II. At Mach 2.8, the ratio is 3.05 for mode III compared with 2.62 for mode I. If the exhaust-nozzle-exit area is made equal to the compressor frontal area, net thrust at Mach 2.8 is reduced 21 percent for mode III and 15 percent for mode I.

#### SUMMARY OF RESULTS

An analytical investigation was made of a hypothetical two-spool turbojet engine having a design compressor pressure ratio of 7.0 and a design inner-turbine inlet temperature of 2500° R. Engine performance and component areas were calculated for three modes of engine operation.

For all three modes, inner-turbine inlet temperature was maintained constant at 2500° R. For mode I, outer-spool mechanical speed was maintained constant at its design value. For mode II operation, inner-spool mechanical speed was maintained constant at its design value. For mode III operation, outer-compressor equivalent speed was maintained constant at 110 percent design for all engine inlet temperatures less than 567° R; for higher inlet temperatures, outer-compressor mechanical speed was maintained constant at 115 percent design.

The following results were obtained:

1. Engine performance with afterburning and with the afterburner inoperative for mode I operation is better than that for mode II over most of the flight range. Mode I thrust values exceed mode II thrust values by as much as 23 percent. The specific-fuel-consumption values for the two modes are about the same, the maximum difference being about 3 percent.

2. Engine performance with afterburning and with the afterburner inoperative for mode III operation is better than that for mode I. Mode III thrust values exceed those for mode I by 6 to 22 percent. Over most of the flight range, the specific fuel consumption for mode III is less than that for mode I, the maximum difference is about 5 percent.

3. The maximum value of inner-spool centrifugal stress is 12 percent higher for mode I than for mode II, while the maximum value of outer-spool centrifugal stress is 12 percent higher for mode II than for mode I.

4. The maximum outer-spool centrifugal stress for mode III is 32 percent higher than that for mode I, while the inner-spool centrifugal stress is the same for modes III and I.

5. At Mach 2.8, the combustor frontal area for modes I and III is 6 and 11.5 percent larger than the compressor frontal area, respectively. For the range of flight conditions considered, the combustor frontal area for mode II is always smaller than the compressor frontal area.

6. The afterburner frontal area exceeds the compressor frontal area by 18.5, 19, and 35 percent for modes I, II, and III, respectively.

7. At Mach 2.36 with the afterburner inoperative, the ratio of exhaust-nozzle-exit area for complete expansion to compressor frontal area is 1.59 for mode I compared with 1.32 for mode II; with afterburning, the ratios are 2.16 for mode I compared with 1.78 for mode II. At Mach 2.8 with the afterburner inoperative, the ratio of exhaust-nozzle-exit area is 2.13 for mode III compared with 1.92 for mode I; with afterburning, the ratios are 3.05 for mode III compared with 2.62 for mode I.

8. The outer and inner compressors are not restricted by their stall-limit lines for any of the operating modes. For all three modes, the outer compressor tends to operate at maximum efficiency while the inner compressor operates at maximum efficiency only at speeds near design.

9. The inner turbine operates very close to its design point over the full range of flight conditions for each operating mode.

10. The outer turbine operates at nearly constant efficiency for modes I and II. During part of the flight range for mode III operation, the outer turbine operates in a reduced-efficiency region close to limiting loading.

Lewis Flight Propulsion Laboratory  
National Advisory Committee for Aeronautics  
Cleveland, Ohio, September 8, 1955

## APPENDIX A

## SYMBOLS

The following symbols are used in this report:

|          |   |
|----------|---|
| A        | area, sq ft   |
| a        | velocity of sound, ft/sec   |
| $C_V$    | velocity coefficient  |
| F        | thrust, lb  |
| f        | fuel-air ratio  |
| g        | standard gravitational acceleration, 32.174 ft/sec <sup>2</sup>                 |
| H        | stagnation enthalpy, Btu/lb   |
| J        | mechanical equivalent of heat, 778.2 ft-lb/Btu                                  |
| M        | Mach number   |
| N        | rotational speed, rpm   |
| P        | total pressure, lb/sq ft  |
| p        | static pressure, lb/sq ft   |
| R        | gas constant, 53.345 ft-lb/(lb)(°R)   |
| sfc      | specific fuel consumption, lb fuel/(hr)(lb thrust)                              |
| T        | total temperature, °R   |
| t        | static temperature, °R  |
| U        | wheel speed, ft/sec   |
| V        | velocity, ft/sec  |
| w        | weight flow, lb/sec   |
| z        | ratio of radius to tip radius   |
| $\gamma$ | ratio of specific heat at constant pressure to specific heat at constant volume |

- $\delta$  ratio of total pressure to NACA standard sea-level pressure,  $P/2116$
- $\eta$  adiabatic efficiency
- $\theta$  ratio of total temperature to NACA standard sea-level temperature,  
 $T/518.7$
- $\rho$  density, slugs/cu ft

## Subscripts:

- an annular
- cr critical
- d design
- f frontal
- h hub
- i inner spool
- j jet
- n net
- o outer spool
- T total conditions
- x axial
- 0 ambient conditions
- 1 outer-compressor inlet
- 2 inner-compressor inlet
- 3 combustor inlet
- 4 inner-turbine inlet
- 5 outer-turbine inlet
- 6 outer-turbine exit
- 6a afterburner inlet



- 7 exhaust-nozzle inlet
- 7a exhaust-nozzle throat
- 8 exhaust-nozzle exit

3820



## APPENDIX B

## MATCHING PROCEDURES

## Inner-Spool Performance

The performance of the inner-spool was found by methods similar to those described in reference 3. Inner-compressor performance was plotted

as  $\frac{(H_3 - H_2) \left( \frac{N_1}{\sqrt{\theta_2}} \right)_d^2}{N_1^2}$  against  $\frac{w_2 N_1}{\delta_3 (P_4/P_3) (N_1/\sqrt{\theta_2})_d}$  for constant values of  $\frac{N_1/\sqrt{\theta_2}}{(N_1/\sqrt{\theta_2})_d}$ . Inner-turbine performance was plotted as

$\frac{(H_4 - H_5) \left( \frac{N_1}{\sqrt{\theta_2}} \right)_d^2}{N_1^2}$  against  $\frac{w_4 N_1}{\delta_4 (N_1/\sqrt{\theta_2})_d}$  for constant values of

$\frac{N_1/\sqrt{\theta_4}}{(N_1/\sqrt{\theta_2})_d}$ . The maps were superimposed to satisfy the matching relations

$$\left( \frac{w_2}{w_4} \right) \frac{(H_3 - H_2)}{N_1^2} = \frac{H_4 - H_5}{N_1^2} \quad (B1)$$

$$\frac{w_2 N_1}{\delta_3 (P_4/P_3)} = \frac{w_4 N_1}{\delta_4} \left( \frac{w_2}{w_4} \right) \quad (B2)$$

Accessory power is assumed to be negligible for matching purposes so that no accessory power term appears in equation (B1). Turbine cooling air would be required for operation at the assigned inner-turbine inlet temperature of 2500° R. The fuel added in the combustor was assumed to compensate for the turbine cooling air bled from the compressor exit so that  $w_2/w_4$  was assigned equal to 1.0. The pressure ratio across the combustor was taken equal to 0.97.

At each match point common to the superimposed maps, the turbine-to compressor-temperature ratio was calculated from

$$\frac{T_4}{T_2} = \left[ \frac{\frac{N_1/\sqrt{\theta_2}}{(N_1/\sqrt{\theta_2})_d}}{\frac{N_1/\sqrt{\theta_4}}{(N_1/\sqrt{\theta_4})_d}} \right]^2 \quad (B3)$$

Other inner-spool quantities were calculated or read from appropriate plots so that inner-spool performance could be plotted as  $w_2\sqrt{\theta_2}/\delta_2$  against  $w_5\sqrt{\theta_5}/\delta_5$  for constant values of  $T_5/T_2$ .

#### Inner-Spool Matching with Outer-Spool Components

Outer-compressor performance was plotted as  $\frac{(H_2 - H_1) \left( \frac{N_o}{\sqrt{\theta_1}} \right)_d^2}{N_o^2}$  and

$T_2/T_1$  against  $w_2\sqrt{\theta_2}/\delta_2$  for constant  $\frac{N_o/\sqrt{\theta_1}}{(N_o/\sqrt{\theta_1})_d}$ . Outer-turbine per-

formance was plotted as  $\frac{(H_5 - H_6) \left( \frac{N_o}{\sqrt{\theta_1}} \right)_d^2}{N_o^2}$  against  $\frac{w_5 N_o}{\delta_5 (N_o/\sqrt{\theta_1})_d}$  for

constant  $\frac{N_o/\sqrt{\theta_5}}{(N_o/\sqrt{\theta_1})_d}$ . The following iteration procedure was used to match

the inner spool with the outer compressor and outer turbine:

- (1) An outer-compressor operating point is assigned. This gives

values of  $\frac{w_2\sqrt{\theta_2}}{\delta_2}$ ,  $\frac{N_o/\sqrt{\theta_1}}{(N_o/\sqrt{\theta_1})_d}$ ,  $\frac{(H_2 - H_1) \left( \frac{N_o}{\sqrt{\theta_1}} \right)_d^2}{N_o^2}$ , and  $T_2/T_1$ .

- (2) A trial value of  $\frac{N_o/\sqrt{\theta_5}}{(N_o/\sqrt{\theta_1})_d}$  is assigned. If the wrong value

is assigned, a contradiction will arise, because specifying an outer-compressor operating point is sufficient to fix the operation of all the remaining components.

(3) A value of  $\frac{w_5 N_o}{\delta_5 (N_o/\sqrt{\theta_1})_d}$  is read from the outer-turbine map for

known values of  $\frac{N_o/\sqrt{\theta_5}}{(N_o/\sqrt{\theta_1})_d}$  and  $\frac{(H_5 - H_6) \left(\frac{N_o}{\sqrt{\theta_1}}\right)_d^2}{N_o^2}$ . Because

$w_1 = w_2 = w_3 = w_4 = w_5$ , the value of  $\frac{(H_2 - H_1) \left(\frac{N_o}{\sqrt{\theta_1}}\right)_d^2}{N_o^2}$  from step (1)

equals  $\frac{(H_5 - H_6) \left(\frac{N_o}{\sqrt{\theta_1}}\right)_d^2}{N_o^2}$ .

(4) A value of  $w_5 \sqrt{\theta_5}/\delta_5$  is calculated from  $\frac{w_5 N_o}{\delta_5 (N_o/\sqrt{\theta_1})_d}$  and  $\frac{N_o/\sqrt{\theta_5}}{(N_o/\sqrt{\theta_1})_d}$ .

(5) A value of  $T_5/T_2$  is read from the inner-spool performance map for known values of  $w_2 \sqrt{\theta_2}/\delta_2$  and  $w_5 \sqrt{\theta_5}/\delta_5$ .

(6) A second value of  $T_5/T_2$ , which depends on the relation between the outer-spool component equivalent speeds, is calculated from

$$\frac{T_5}{T_2} = \frac{\left[ \frac{N_o/\sqrt{\theta_1}}{(N_o/\sqrt{\theta_1})_d} \right]^2}{\frac{N_o/\sqrt{\theta_5}}{(N_o/\sqrt{\theta_1})_d}} \quad (B4)$$

If this does not equal the value from step (5), steps (2) through (6) are repeated until agreement is reached.

All the two-spool gas-generator quantities required to compute the pumping characteristics may now be calculated or read from appropriate plots. The pumping characteristics are represented by plots of  $T_4/T_1$ ,  $T_6/T_1$ ,  $P_6/P_1$ ,  $N_1/\sqrt{\theta_1}$ , and  $f/\theta_1$  against  $w_1\sqrt{\theta_6}/\delta_6$  for constant values of  $N_0/\sqrt{\theta_1}$ .

## REFERENCES

1. Dugan, James F., Jr.: Effect of Design Over-All Compressor Pressure Ratio Division on Two-Spool Turbojet-Engine Performance and Geometry. NACA RM E54F24a, 1954.
2. Heaton, Thomas R., Forrette, Robert E., and Holeski, Donald E.: Investigation of a High-Temperature Single-Stage Turbine Suitable for Air Cooling and Turbine Stator Adjustment. I - Design of Vortex Turbine and Performance with Stator at Design Setting. NACA RM E54C15, 1954.
3. Dugan, James F., Jr.: Two-Spool Matching Procedures and Equilibrium Characteristics of a Two-Spool Turbojet Engine. NACA RM E54F09, 1954.
4. Turner, L. Richard, and Bogart, Donald: Constant-Pressure Combustion Charts Including Effects of Diluent Addition. NACA Rep. 937, 1949. (Supersedes NACA TN's 1086 and 1655.)

3820

CW-4

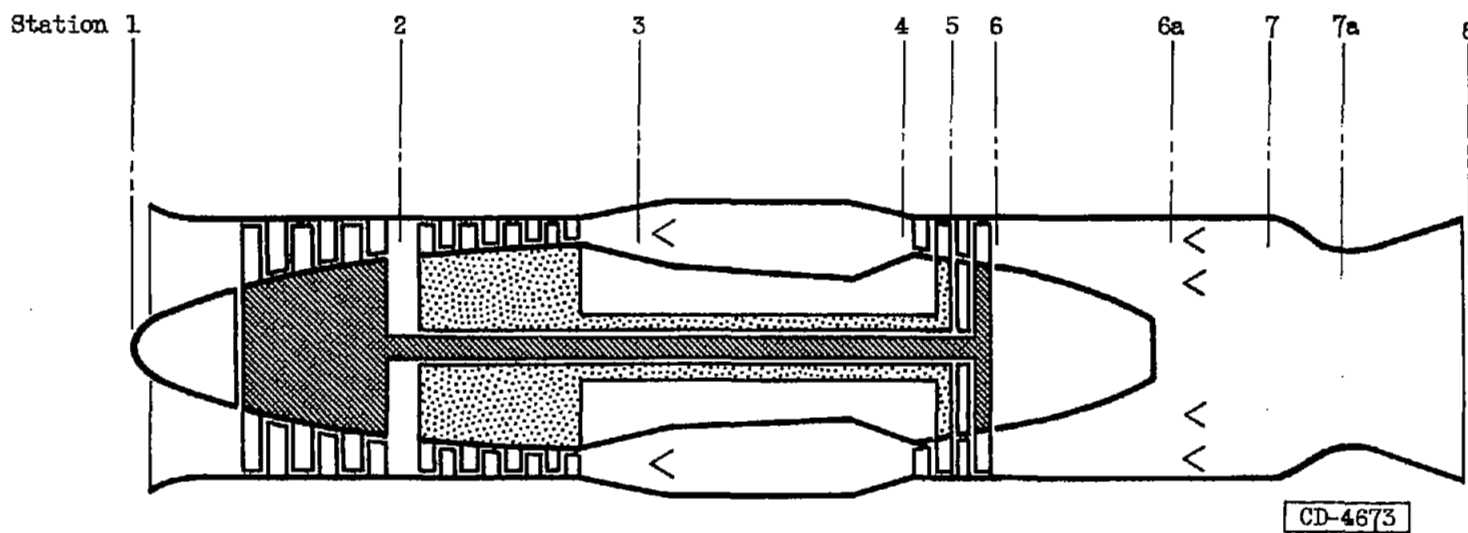
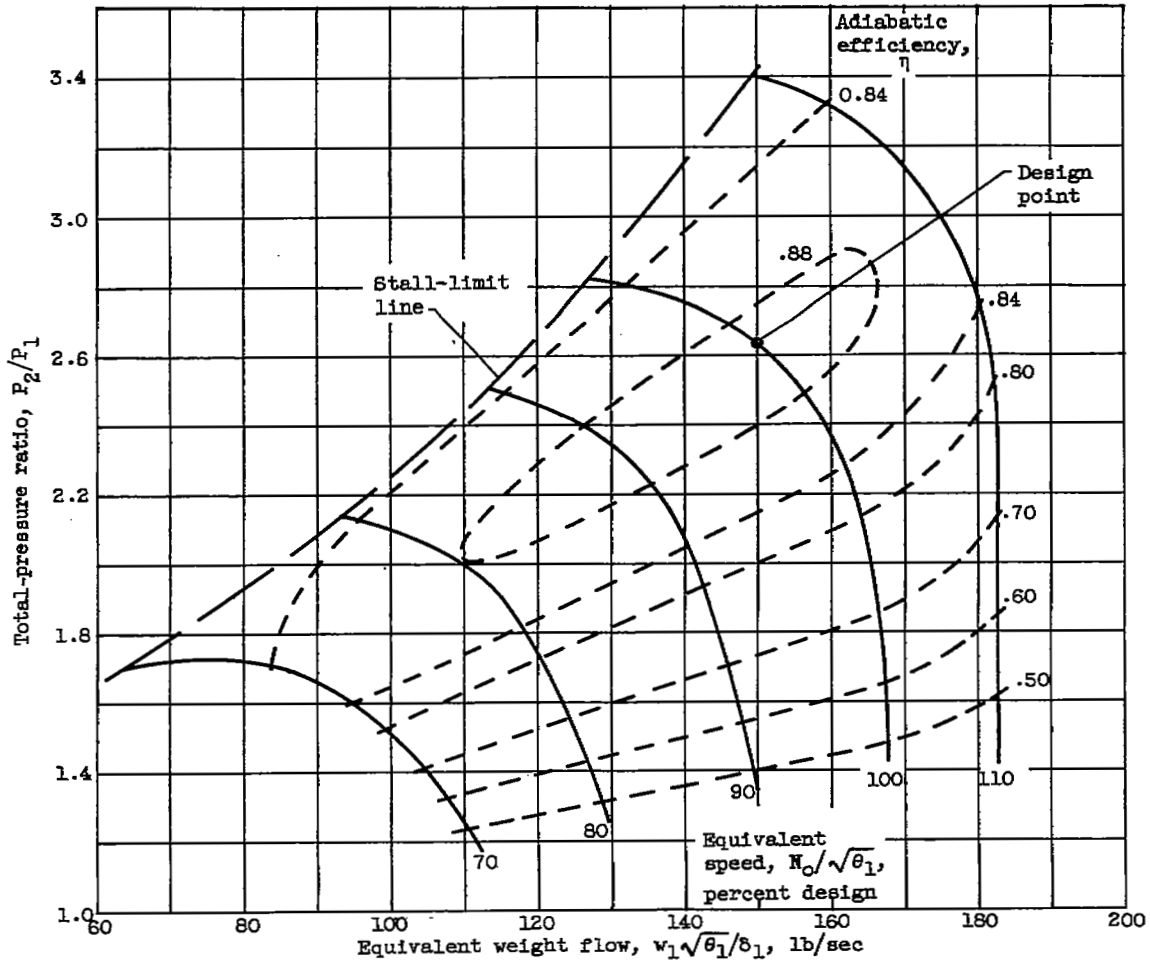


Figure 1. - Cross section of two-spool turbojet engine.

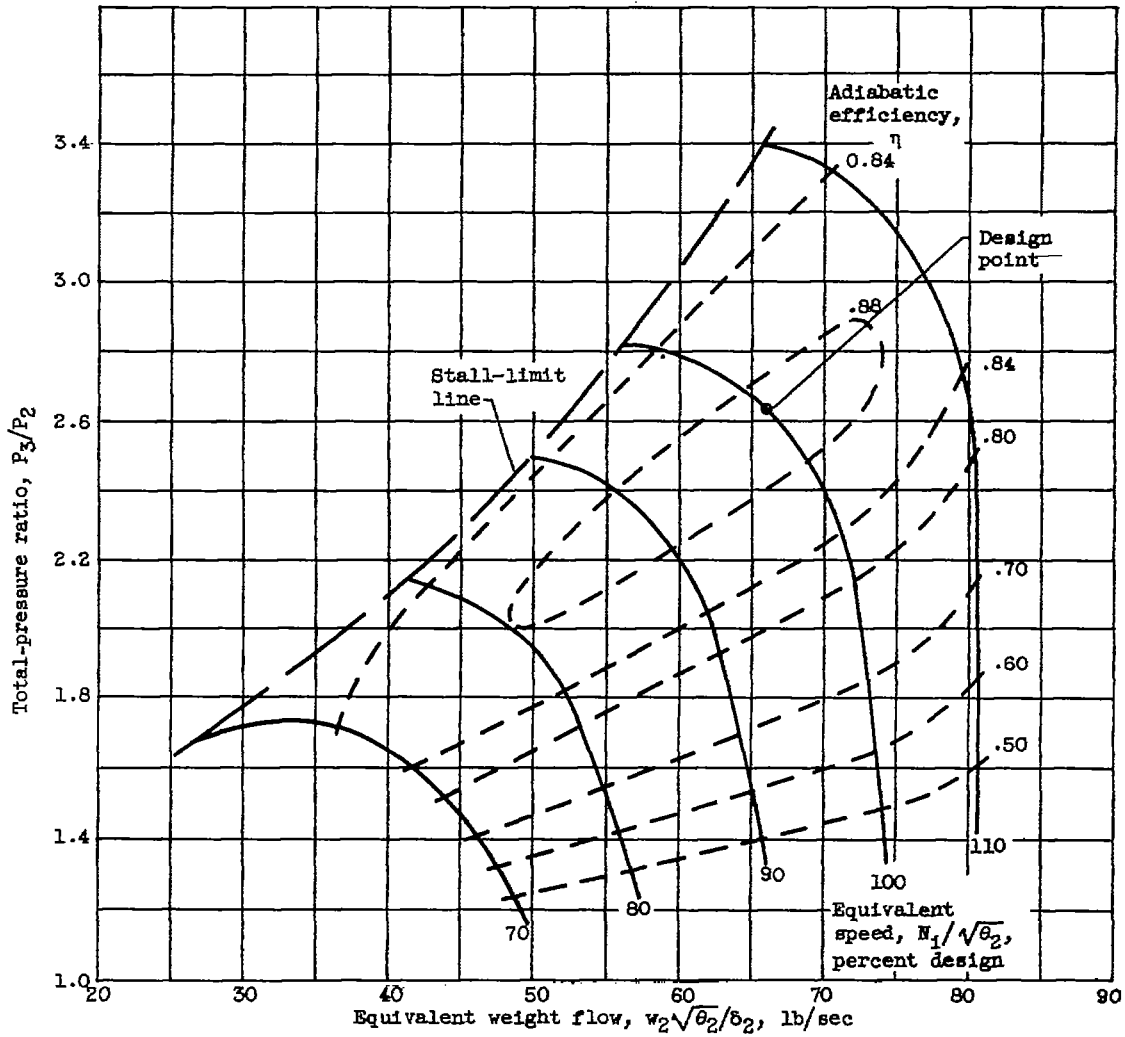
3820

CW-4 back



(a) Outer compressor.

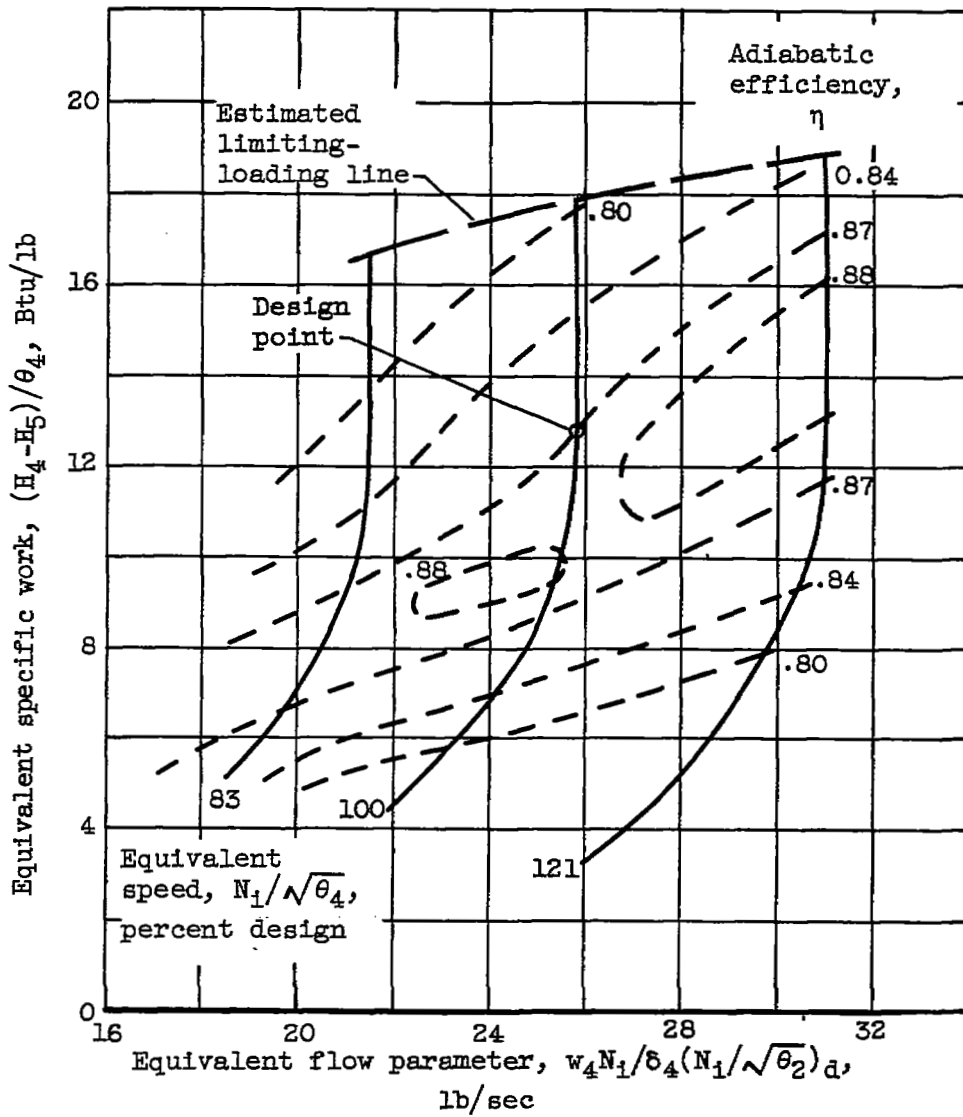
Figure 2. - Component performance maps of two-spool turbojet.



(b) Inner compressor.

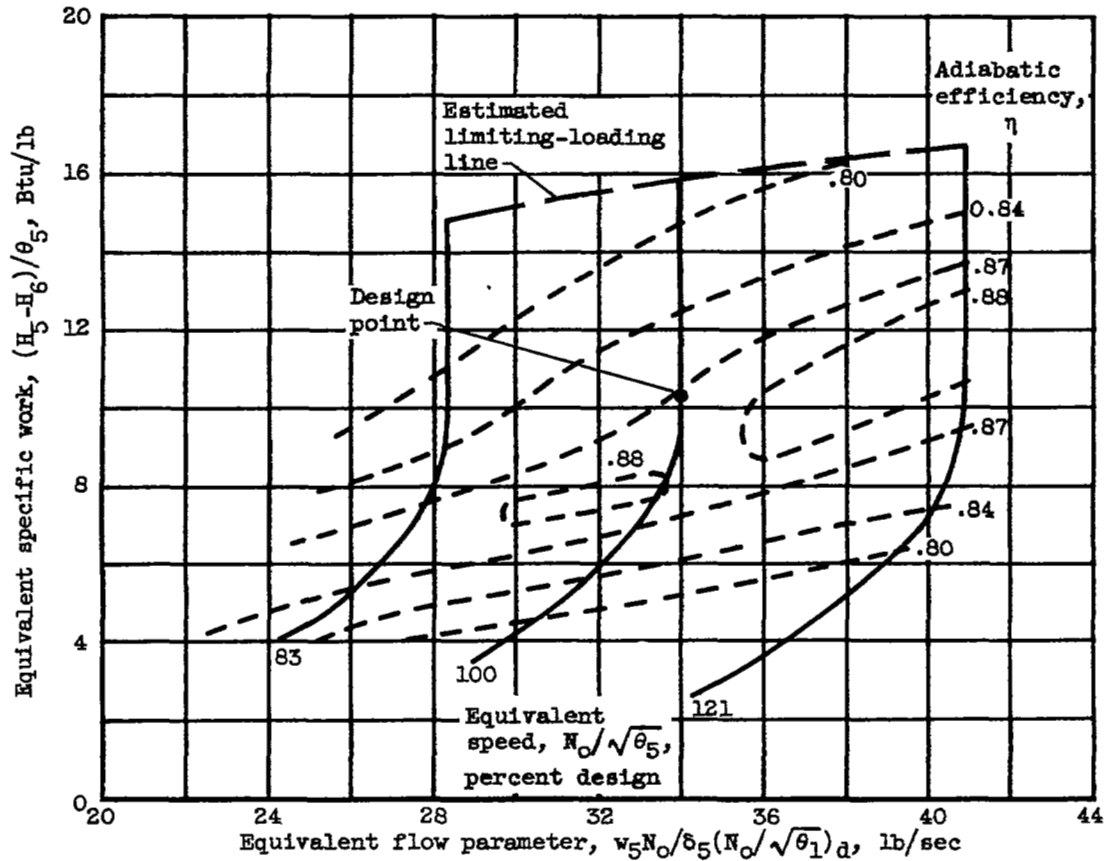
Figure 2. - Continued. Component performance maps of two-spool turbojet.

3820



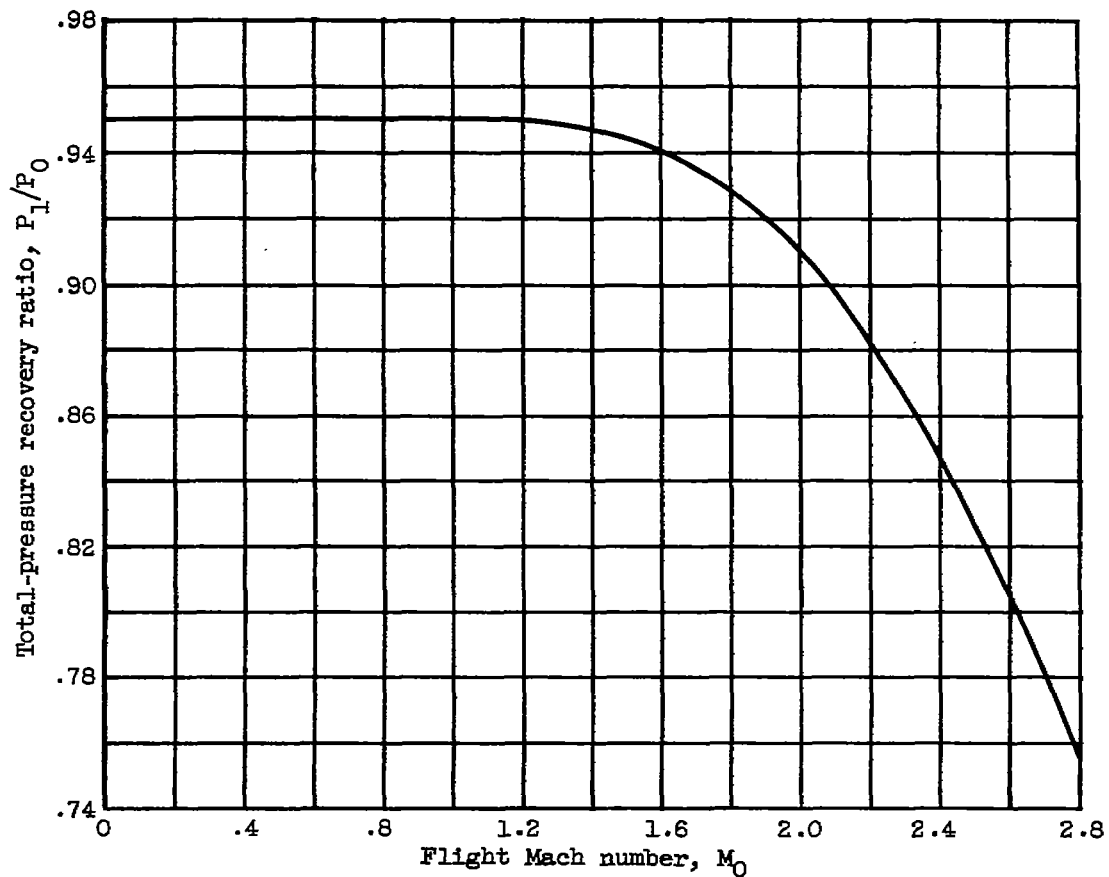
(c) Inner turbine.

Figure 2. - Continued. Component performance maps of two-spool turbojet.



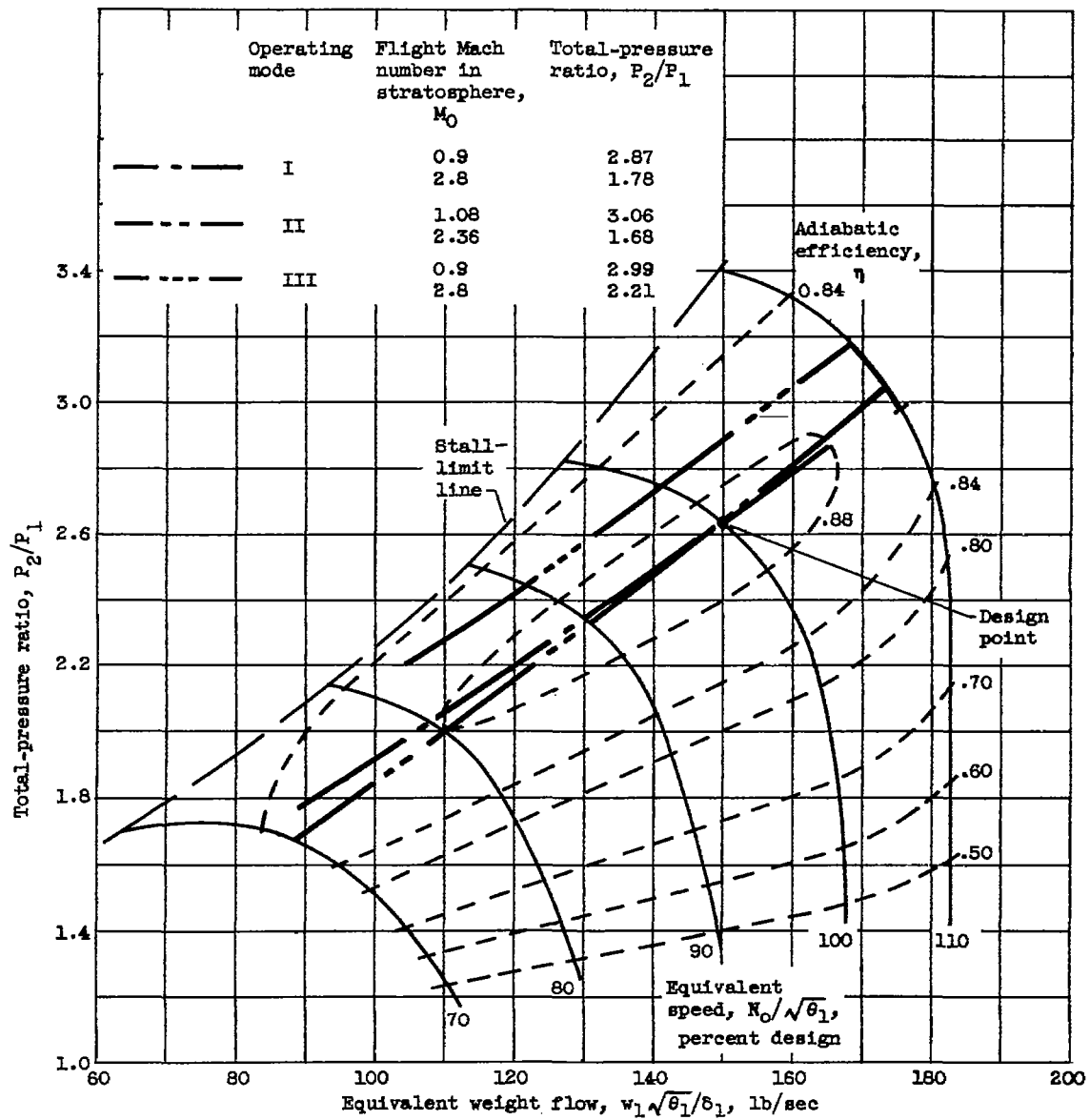
(d) Outer turbine.

Figure 2. - Continued. Component performance maps of two-spool turbojet.



(e) Inlet.

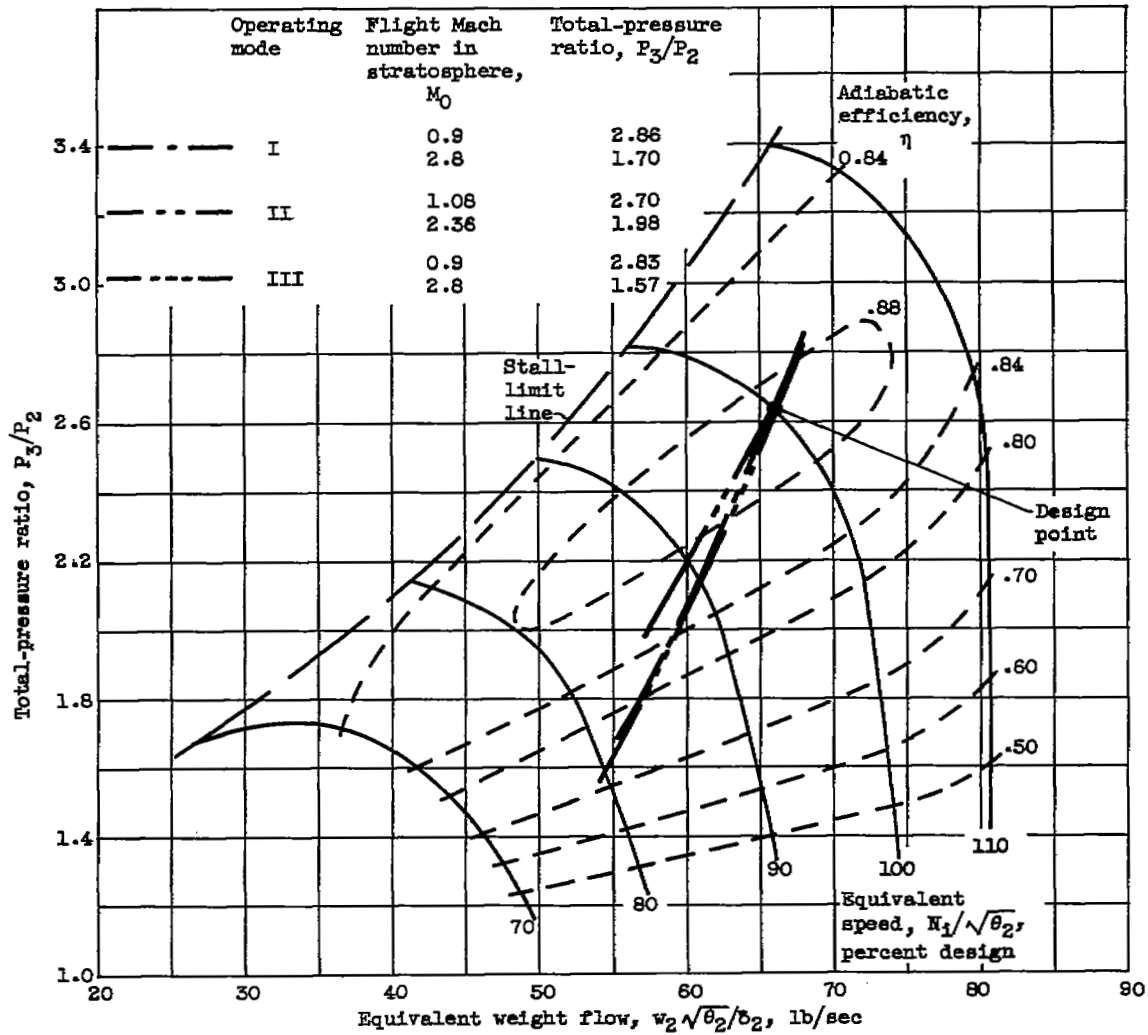
Figure 2. - Concluded. Component performance maps of two-spool turbojet.



(a) Outer-compressor performance map.

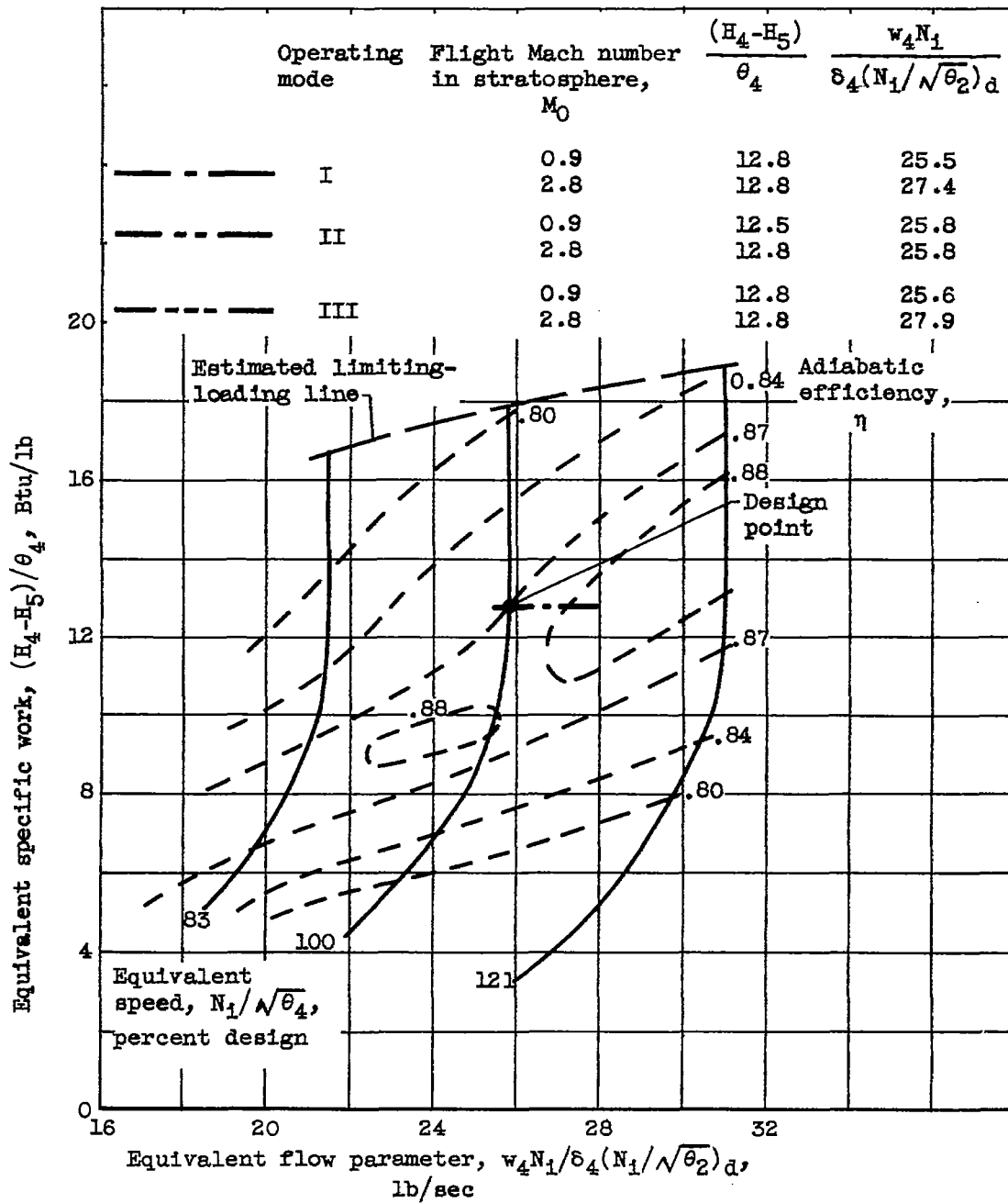
Figure 3. - Operating lines for three modes of operation.

3820  
CW-5



(b) Inner-compressor performance map.

Figure 3. - Continued. Operating lines for three modes of operation.

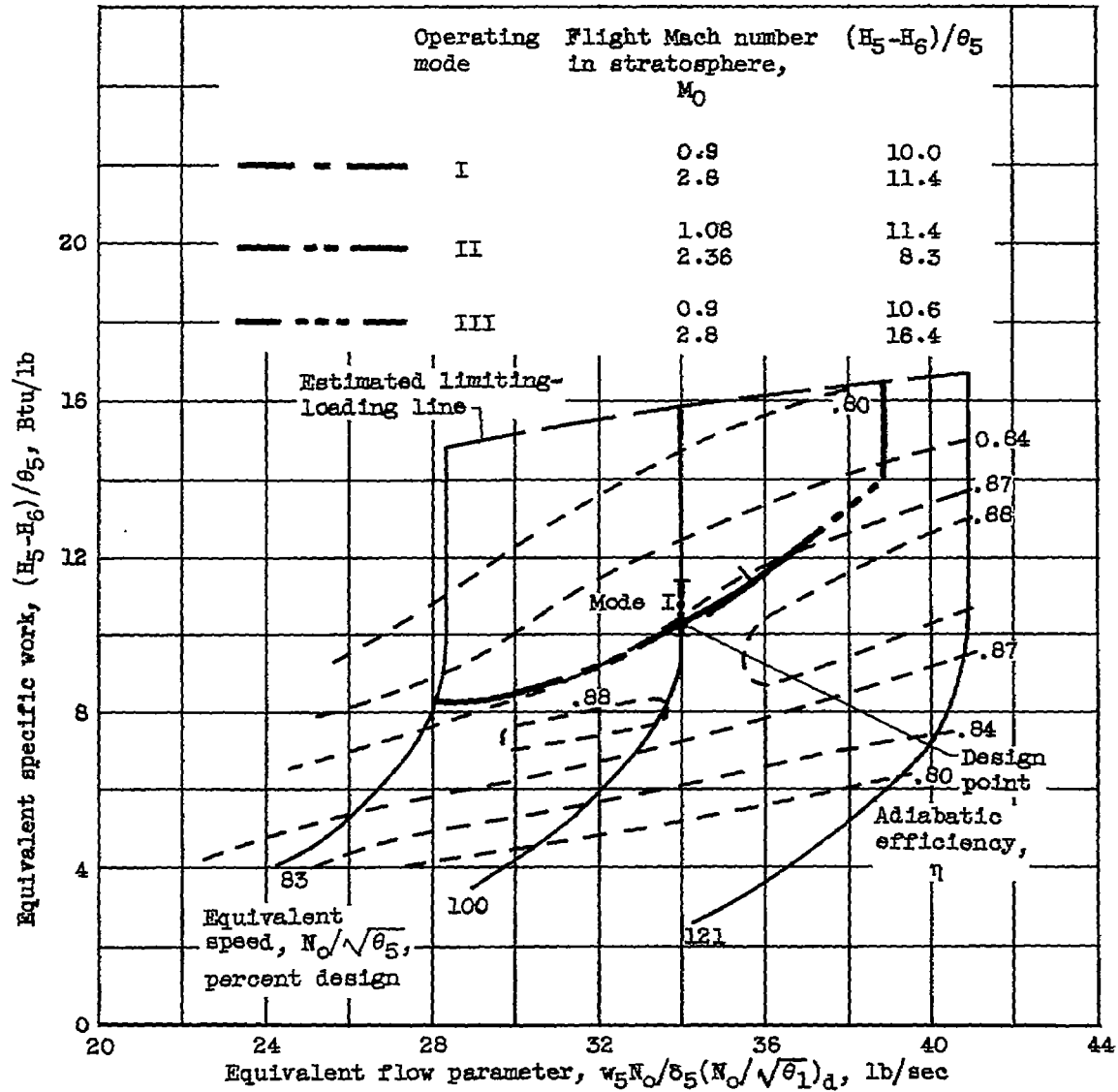


(c) Inner-turbine performance map.

Figure 3. - Continued. Operating lines for three modes of operation.

5820

CW-5 back



(d) Outer-turbine performance map.

Figure 3. - Concluded. Operating lines for three modes of operation.

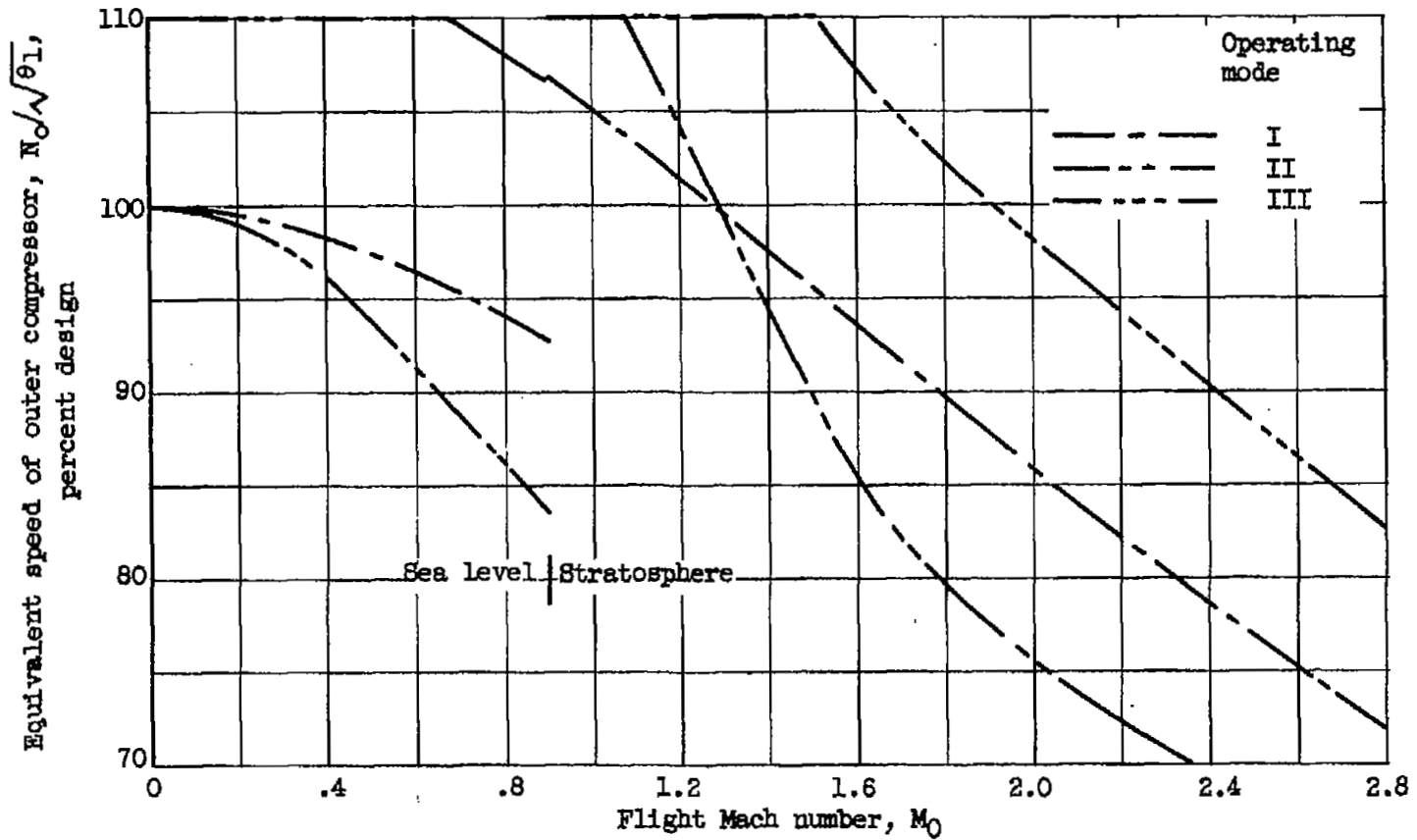
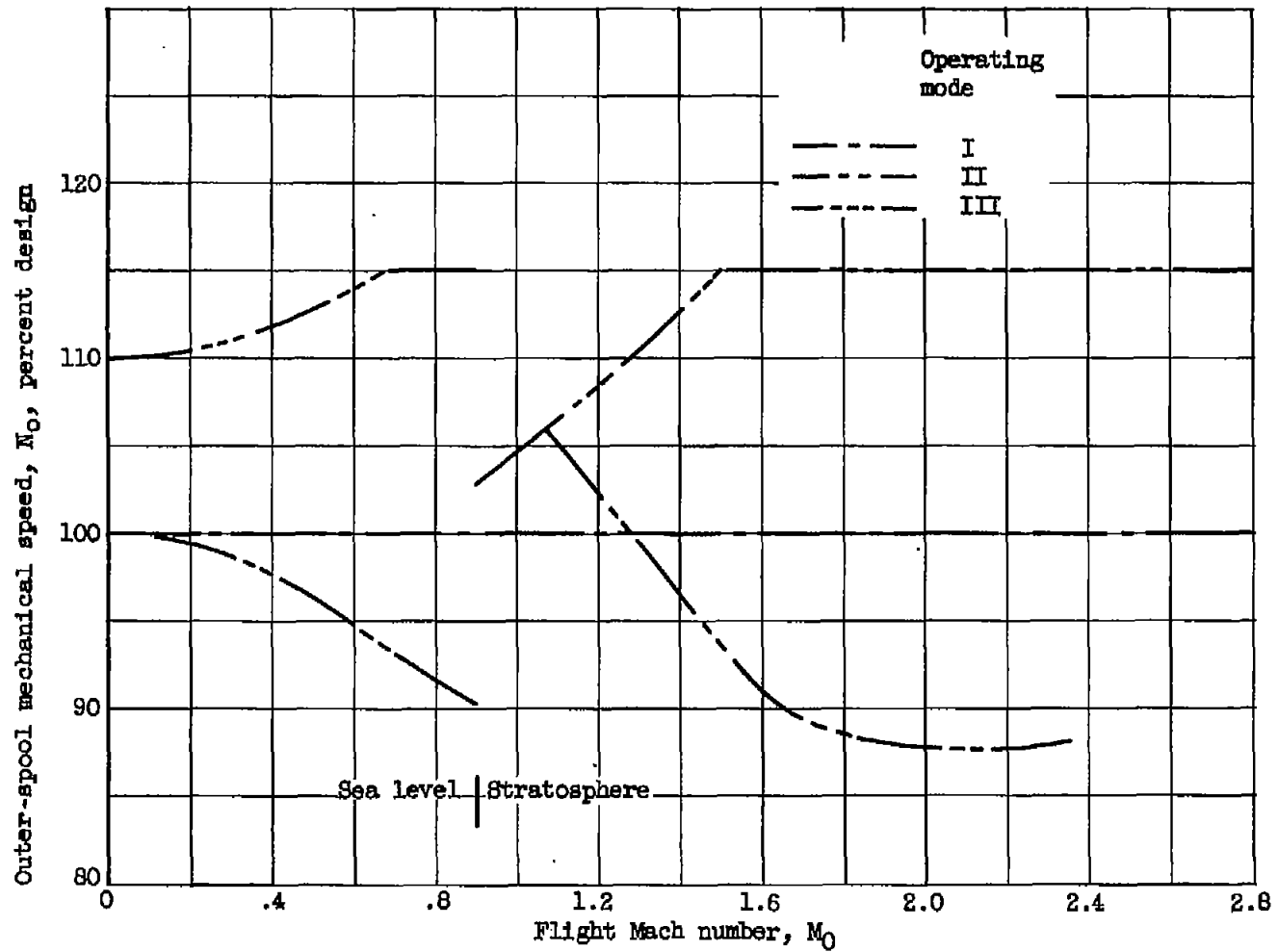
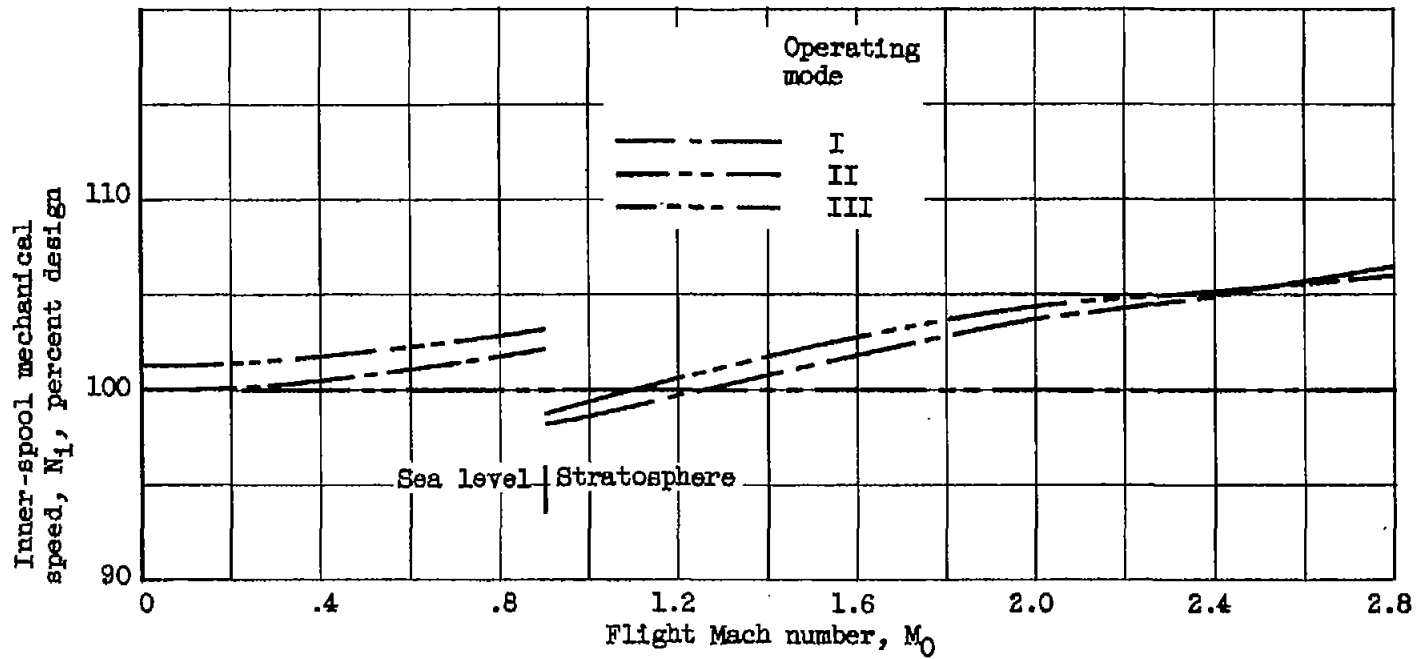


Figure 4. - Variation of outer-compressor equivalent speed with flight Mach number for three modes of operation.



(a) Outer-spool.

Figure 5. - Variation of mechanical speed with flight Mach number for three modes of operation.



(b) Inner-spool.

Figure 5. - Concluded. Variation of mechanical speed with flight Mach number for three modes of operation.

3820

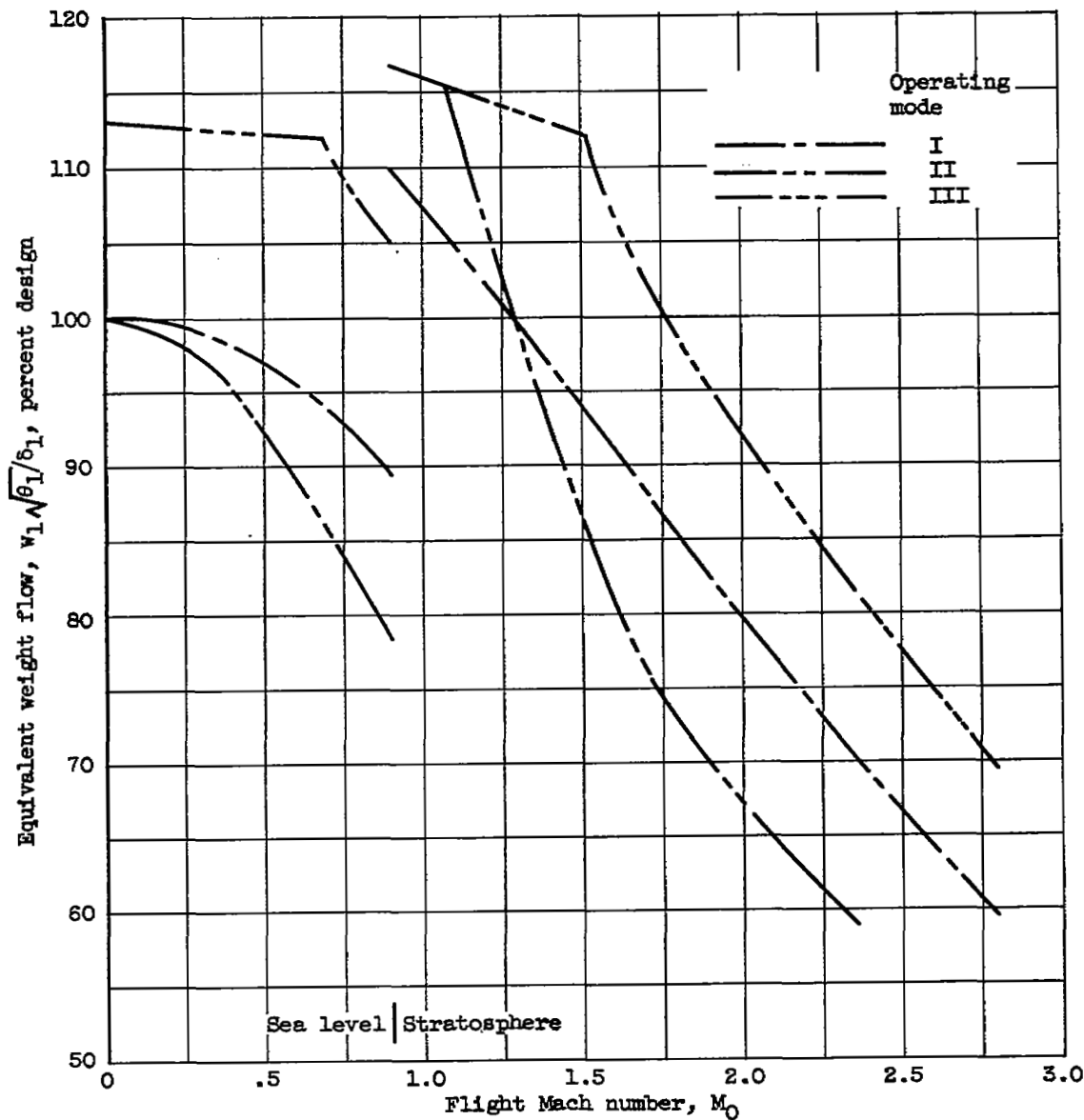
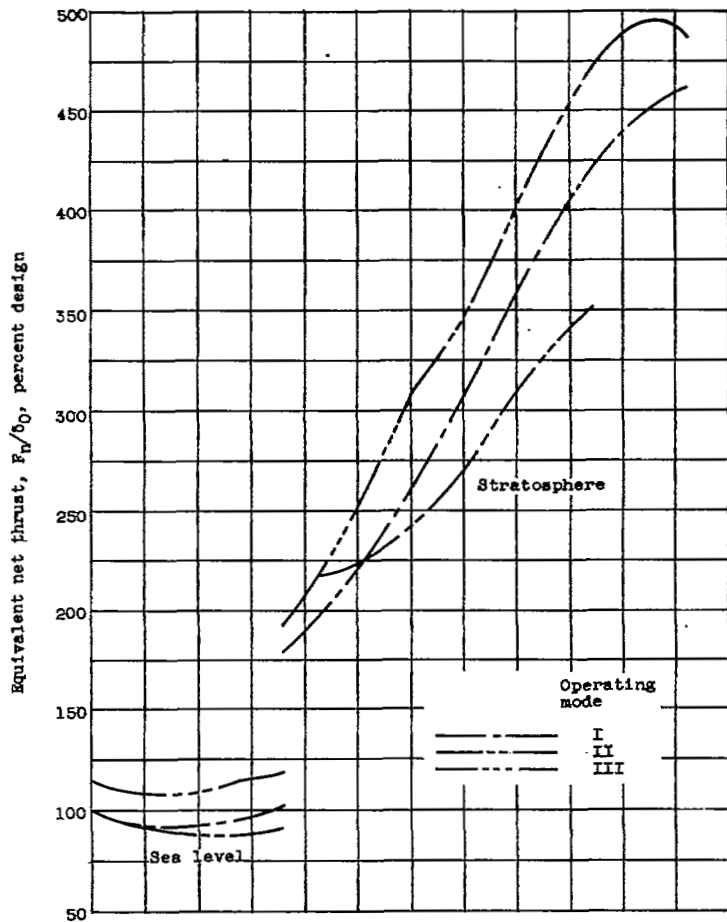
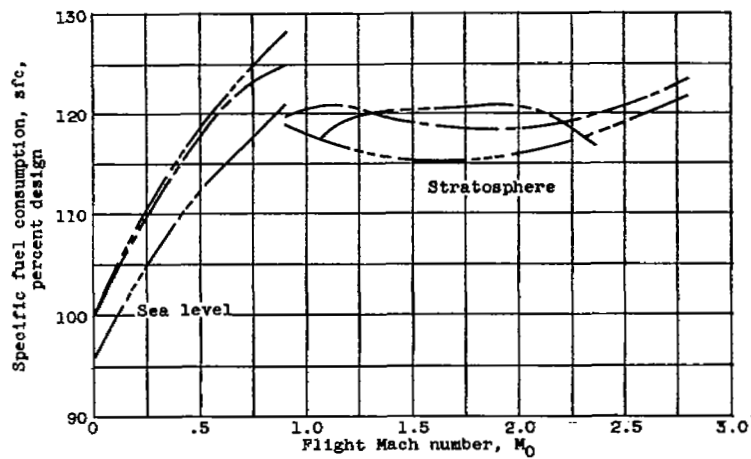


Figure 6. - Variation of engine equivalent weight flow with flight Mach number for three modes of operation.

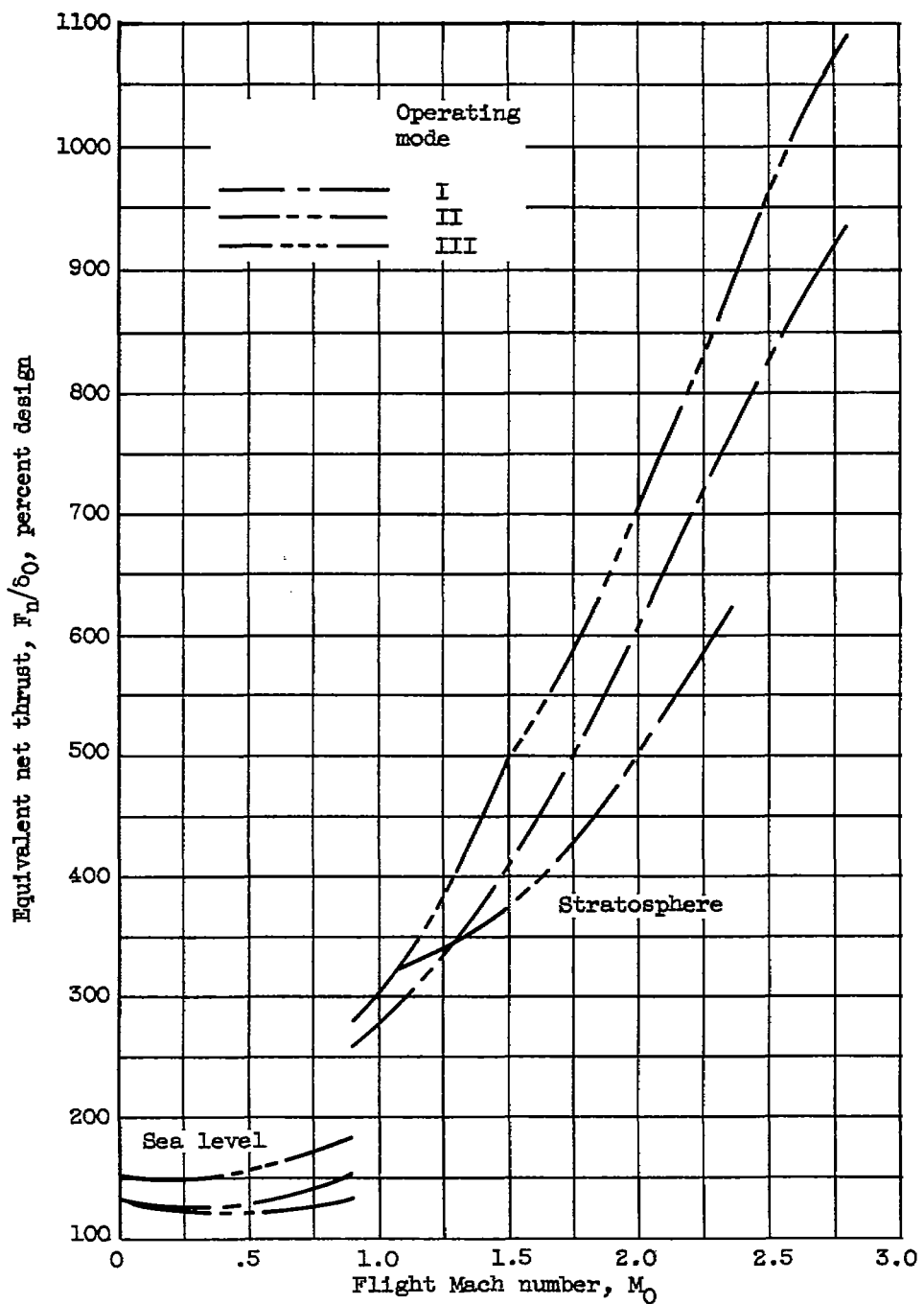


(a) Equivalent net thrust.



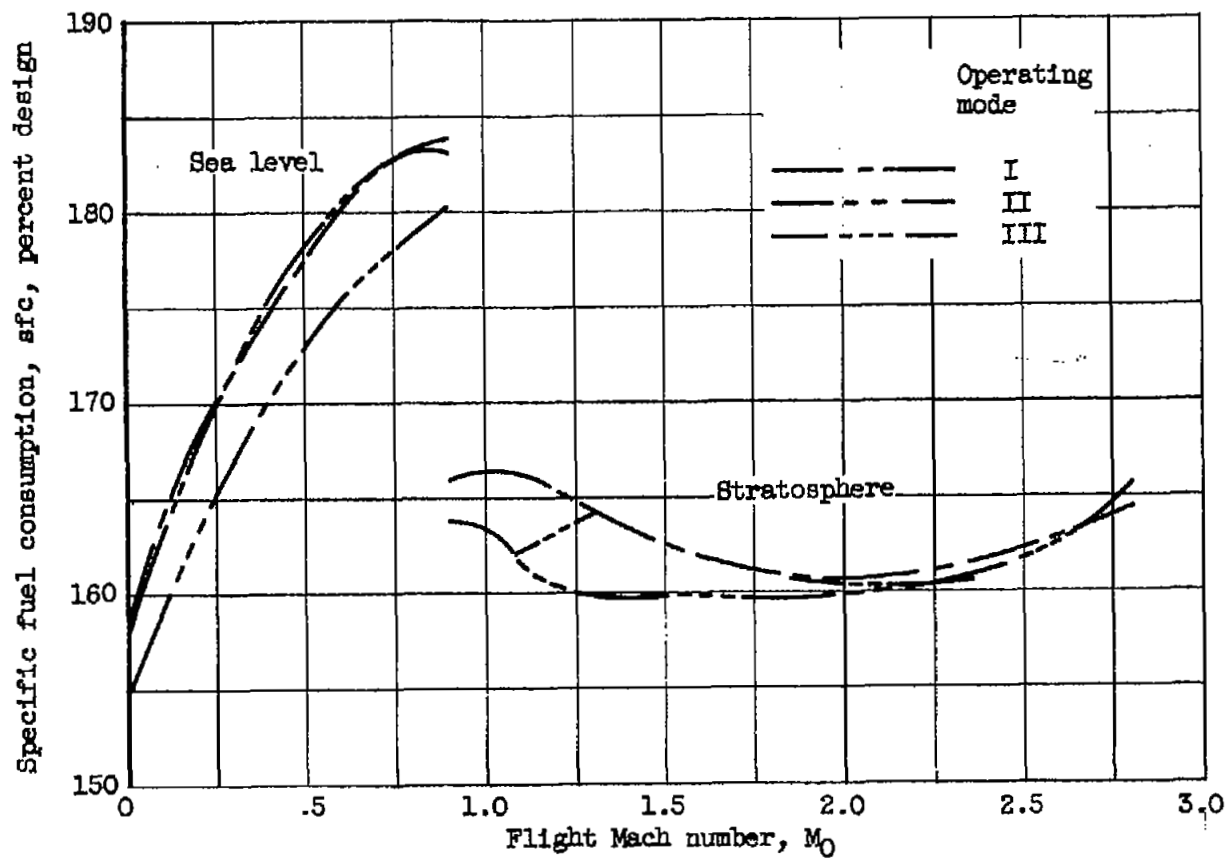
(b) Specific fuel consumption.

Figure 7. - Two-spool performance with afterburner inoperative for three modes of operation.



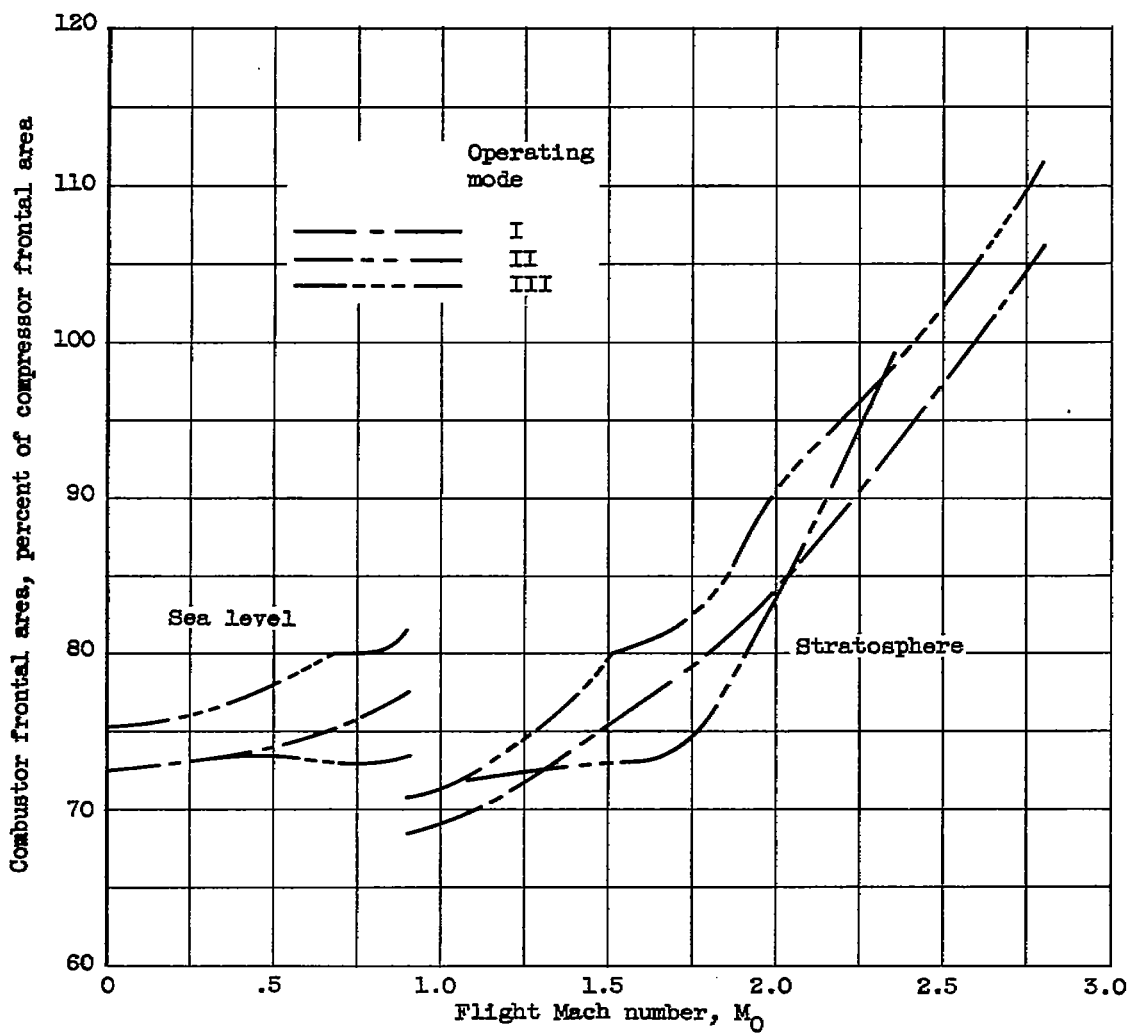
(a) Equivalent net thrust.

Figure 8. - Two-spool performance with afterburning for three modes of operation.



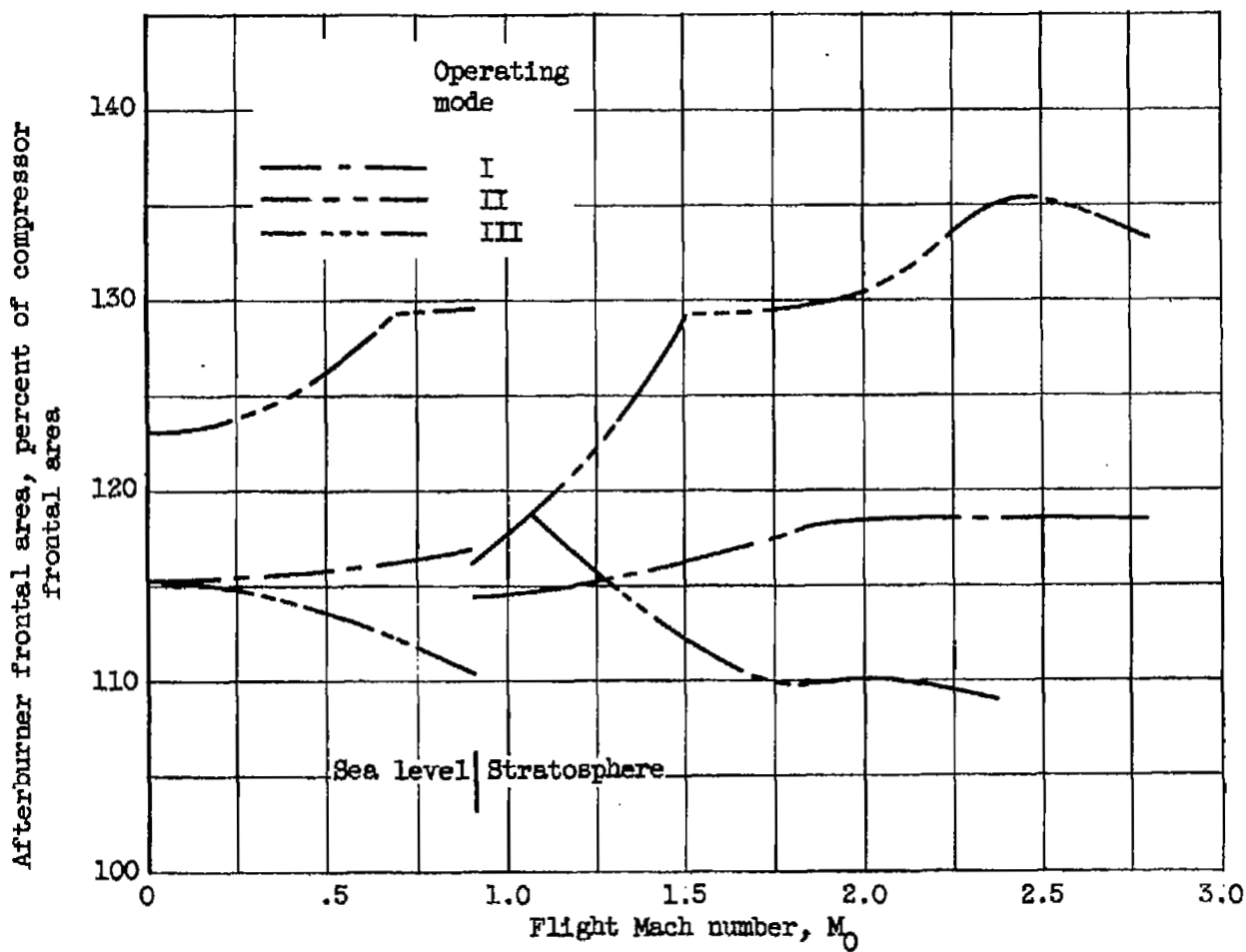
(b) Specific fuel consumption.

Figure 8. - Concluded. Two-spool performance with afterburning for three modes of operation.



(a) Combustor frontal area.

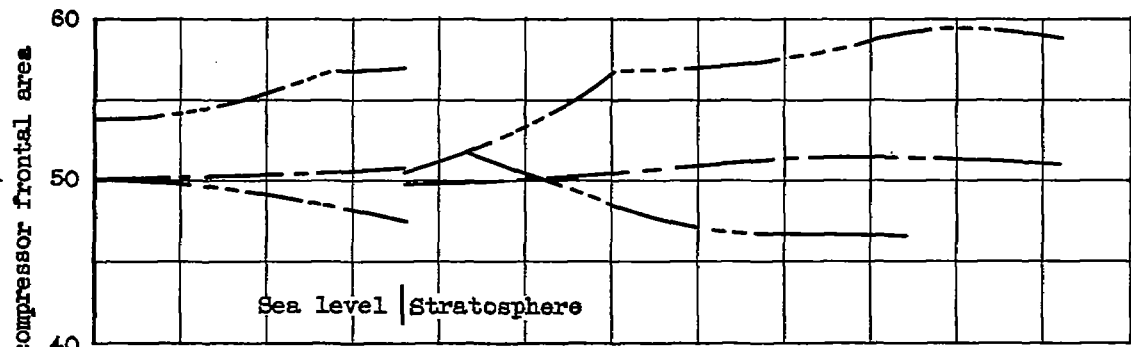
Figure 9. - Variation of frontal areas with flight Mach number for three modes of operation.



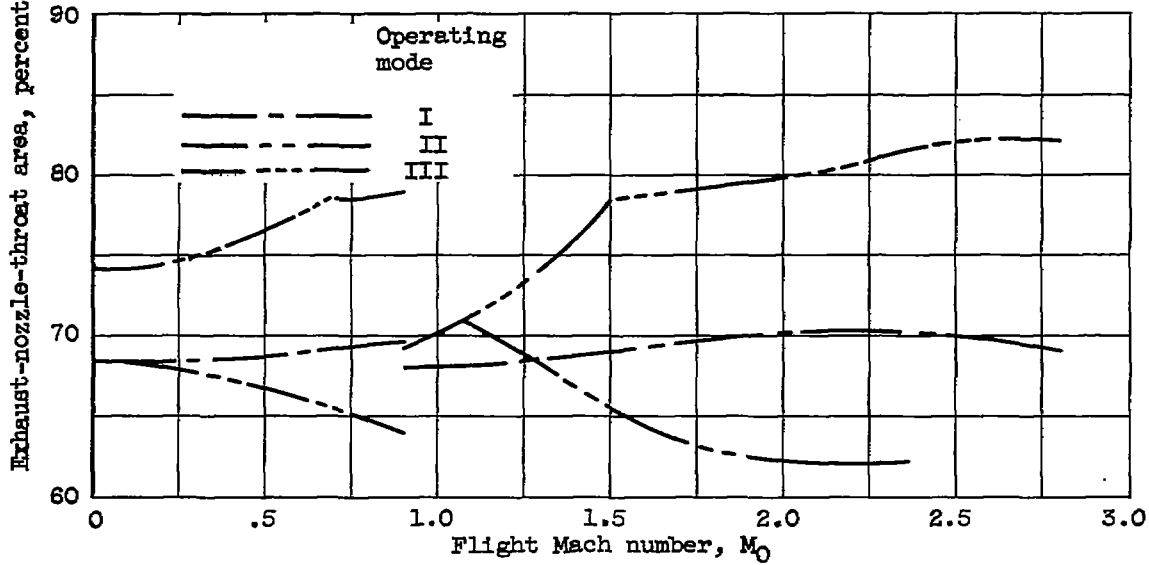
(b) Afterburner frontal area.

Figure 9. - Concluded. Variation of frontal areas with flight Mach number for three modes of operation.

3820

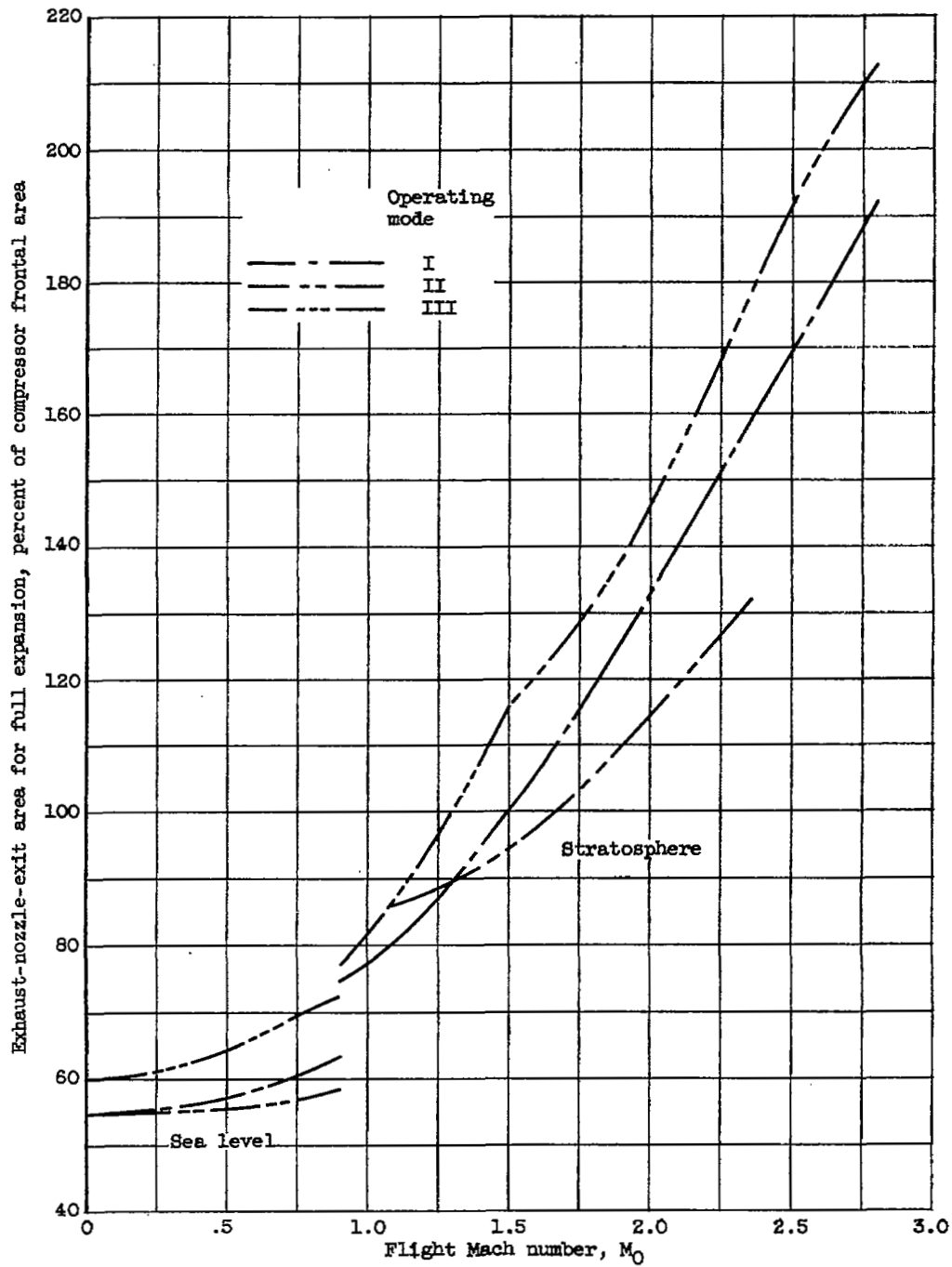


(a) With afterburner inoperative.



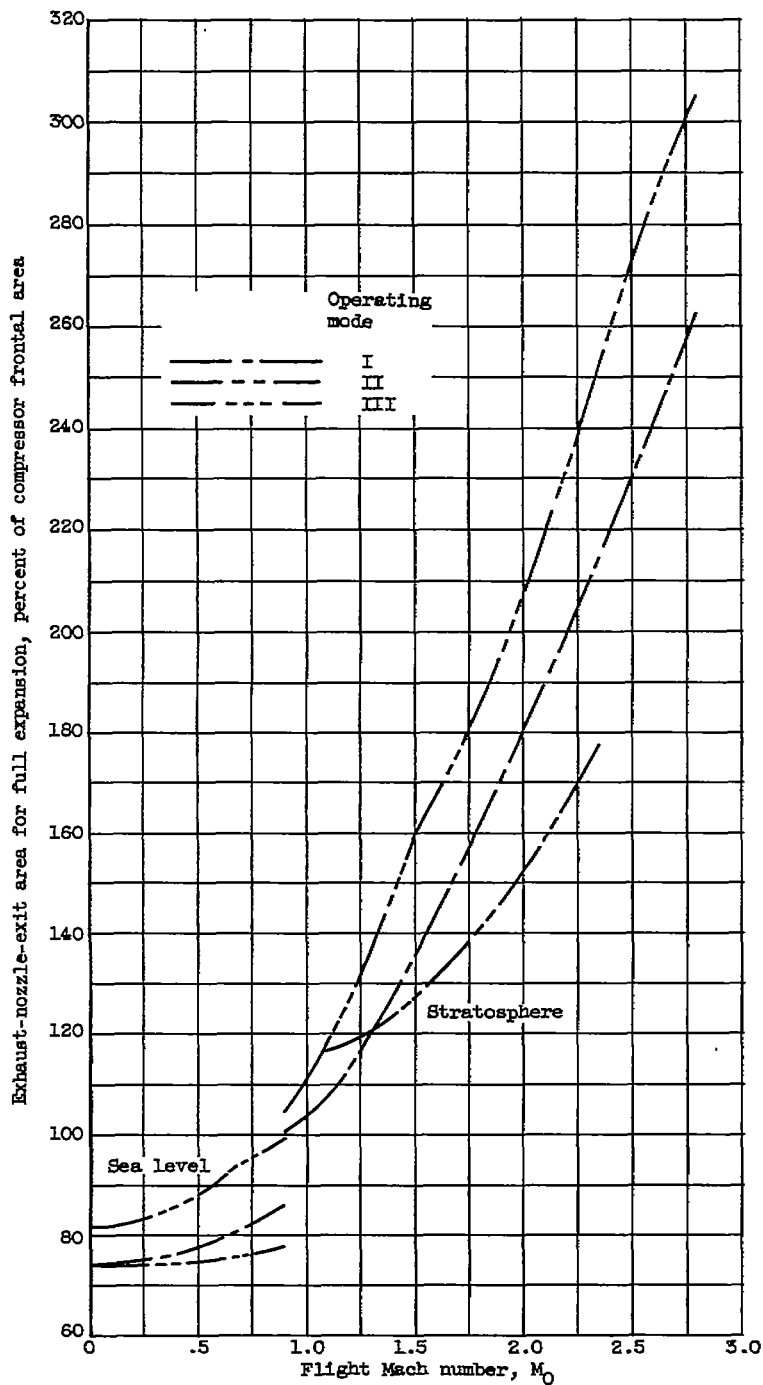
(b) With afterburning.

Figure 10. - Variation of exhaust-nozzle-throat area with flight Mach number for three modes of operation.



(a) With afterburner inoperative.

Figure 11. - Variation of exhaust-nozzle-exit area for full expansion with flight Mach number for three modes of operation.



(b) With afterburning.

Figure 11. - Concluded. Variation of exhaust-nozzle-exit area for full expansion with flight Mach number for three modes of operation.

NASA Technical Library



3 1176 01436 5200

~~CONFIDENTIAL~~